공학 박사 학위 논문

Non-classical deposition of silicon thin film during chemical vapor deposition

비고전적 박막성장을 통한 화학 기상 증착에서의 실리콘 단결정 성장

2016년 8월

서울대학교 대학원

재료공학부

정재수

Abstract

Non-classical deposition of silicon thin film during chemical vapor deposition

Jae-soo, Jung

Department of Material Science and Engineering

The Graduate School

Seoul National University

Silicon thin film have been extensively used in electrical devices for thin film transistors (TFTs) and silicon thin film based solar cells. Until now, formation of thin films and nanostructures explained by classical crystal growth based on atomic or molecules growth. However, many puzzling phenomena and problem generated in the growth of films and

nanostructure, cannot be explained by this classical growth mechanism. By the reason, non-classical crystallization, where crystals grow by the building block of nanoparticles, has become a significant issue not only in solution but also in the gas phase synthesis such as chemical vapor deposition (CVD). In the various CVD processes, the generation of charged nanoparticles (CNPs) in the gas phase has been persistently reported. Many evidences supporting that these CNPs are the building block of thin films and nanostructures were reported. According this new understanding of non-classical crystallization, many thin films and nanostructures which had been believed to grow by individual atoms or molecules turned out to grow by the building block of CNPs.

In this study, the deposition behavior of silicon films by Radio frequency plasma enhanced chemical vapor deposition (RF-PECVD) was studied by the non-classical crystallization, where the growth unit of deposition is a nanoparticles generated in the gas phase of the reactor. According to the non-classical crystallization, the liquid-like property of particles is increased with increasing the amount of charge of particles. To investigate the behavior of particles in the RF-CVD reactor, nanoparticles were observed by transmission electron microscope (TEM) and the deposition rate of films was measured. The behavior of particles which were captured on TEM grid depended by the substrate bias and the conductivity of substrate due to difference of the amount of the charge of

particles. Also, the deposition rate of films was changed by conductivity of the substrates and substrate bias. Using the liquid-like property of charged nanoparticles (CNPs), homo-epitaxial growth could be successfully deposited on a silicon wafer at 550 ℃ under the processing condition where multiply CNPs could be selectively deposited.

The deposition behavior of silicon films by hot wire chemical vapor deposition (HWCVD) was also approached by non-classical crystallization. Using the liquid-like property of small CNPs, homo-epitaxial growth as thick as ~ 150 nm could be successfully grown on a silicon wafer at 600oC under the processing condition where CNPs as small as possible could be supplied steadily. The size of CNPs turned out to be an important parameter in the microstructure evolution of thin films.

Keywords

Silicon thin film; radio frequency plasma enhanced chemical vapor deposition; hot wire chemical vapor deposition; epitaxial growth; non-classical crystallization

Student number

2011-20668

Contents

List of Figures

(a) low magnification TEM image of films, (b) HRTEM image of the silicon film at middle part, and (c) HRTEM image of the interfacial region between silicon wafer and silicon film.

Fig. 11. TEM cross section images of the silicon films on (100) silicon wafer with -1000 V. (a) low magnification TEM image of films, (b) HRTEM image of the silicon film at middle part, and (c) HRTEM image of the interfacial region between silicon wafer and silicon film.

Fig. 12. TEM cross section images of the silicon films on (100) Germanium wafer without bias. (a) HRTEM image of the silicon film of the interfacial region between silicon wafer and silicon film, and (c) HRTEM image at middle part of film

Fig. 13. TEM cross section images of the silicon films on (100) Germanium wafer with -1000 V. (a) HRTEM image of the silicon film of the interfacial region between silicon wafer and silicon film, and (c) HRTEM image at middle part of film

Fig. 14. Measured mass distributions of negatively charged carbon clusters extracted from the hot filament reactor using gas mixtures of 1%CH_4-99%H_2, 1.5%CH_4-98.5%H_2, 3%CH_4-97%H_2, and 5%CH_4-95%H_2

Fig. 15. SEM images of diamond films deposited *in situ* during the measurement of the mass distribution of CNPs at 2100°C wire temperature and 800 Pa reactor pressure: (a) 1%CH_4–

Fig. 16 Schematic of experimental set-up of the HWCVD reactor.

Fig, 17, TEM image of initial silicon charged nanoparticles deposited on the TEM grid membrane for 10 sec after delay times of (a) 0 min and (b) 5 min and (c) 15 min.

Fig 18. Schematics of experimental deposition conditions of silicon films. (a) Normal deposition without delay time, (b) deposition with delay time, (c) after delay time for 5 min, 6 times of cyclic deposition process for 30 sec, and (d) 6 times of cyclic deposition process for 30 sec without delay time.

Fig. 19. TEM cross section images of the silicon film deposited on (100) silicon wafer under the normal condition without delay time. (a) Low magnification TEM image, (b) HRTEM image of the upper dark region, and (c) HRTEM image of the interfacial region between the silicon wafer and the lower dark region

Fig. 20. TEM cross section images of the silicon film deposited on (100) silicon wafer under the condition of Figure 2(d) with 6 times of the cyclic deposition process for 30 sec. (a) Low magnification TEM image of films, (b) HRTEM image of the upper gray layer, and (c) HRTEM image of the interfacial region between the silicon wafer and the film.

List of Tables

Chapter 1. Introduction

Part 1. Background and purpose of this study

1. Non-classical crystallization

The theory of classical crystal growth was established based on the concept that the building block of crystals should be individual ions, atoms or molecules. However, there have been some experimental results, which cannot be properly explained by this classical mechanism. Rather such experimental results strongly imply that crystals should grow by the building block of nanoparticles, whose way of crystal growth is called 'non-classical crystallization'.[1-5] Recently, non-classical crystallization was confirmed by in-situ transmission electron microscope (TEM) observations. Although non-classical crystallization is a relatively[6, 7] new and revolutionary concept in crystal growth, it has now become so established that a few related books have been published and its tutorial and technical sessions have been included respectively in the spring meetings of Materials Research Society (MRS) and European Materials Research Society (EMRS) in 2014. With the establishment of non-classical crystallization, many crystals that were believed to grow by atomic, molecular, or ionic entities turn out to grow actually by nanoparticles.

Non-classical crystallization can be applied to crystal growth not only in solution but also

in the gas phase synthesis of thin films and nanostructures by chemical vapor deposition (CVD) and physical vapor deposition (PVD). Hwang et al.[8-11] studied extensively the non-classical crystallization in the CVD process, publishing more than 80 SCI papers. They suggested that the electric charge carried by the nanoparticles played a critical role, by which the growth of thin films and nanostructures by the building block of nanoparticles is made possible. This is why they called this new growth mechanism in the gas phase synthesis 'theory of charged nanoparticles (TCN)'. According to this theory, charged nanoparticles (CNPs), which are spontaneously generated in the gas phase in most CVD processes, become the building block of thin films and nanostructures. If nanoparticles are neutral, they undergo random Brownian coagulation. If nanoparticles are charged, however, they deposit as dense films without voids. This is because CNPs are liquid-like and undergo self-assembly.

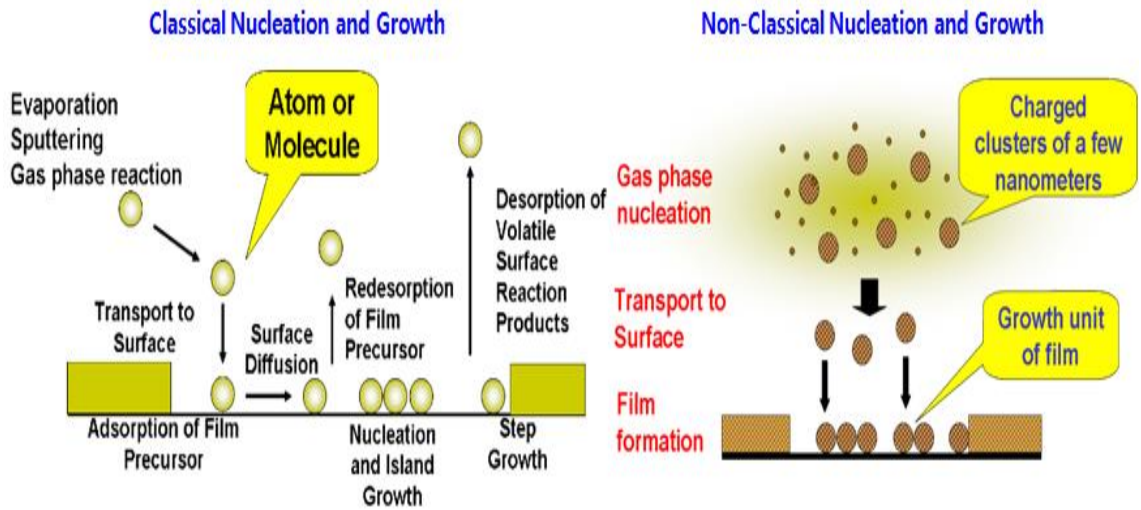

Fig.1. Schematic for the classical crystallization and non-classical crystallization.

The first reason why this new growth mechanism has been unknown would be that CNPs are invisible because their size is much smaller than the wavelength of visible light. The second reason would be that it is difficult to believe that CNPs can be the building block for the evolution of the dense films and nanostructures. The generation of CNPs in the gas phase was experimentally confirmed in many CVD processes synthesizing such as diamond [12, 13], ZrO_2 [14],Si [15], carbon nanotubes [16, 17], ZnO nanowires [18] and silicon nanowires [19]. The reason why these CNPs can be the building block of thin films and nanostructures is that the charge weakens the bond strength and make nanoparticles liquid-like.

The thin film growth by CVD is explained in the text book as follows. Atoms or molecules are formed on the growing surface or in the gas phase as a result of chemical reactions of reactant gases. Those atoms or molecules are then adsorbed on a terrace, diffuse to a ledge and becomes incorporated in the crystal lattice at the kink, which is called the terrace, ledge and kink (TLK) model [20, 21]. This mechanism is called 'classical crystal growth mechanism'. Normally, a ledge of monoatomic height is regarded as a kink because the ledge is disordered or rough, consisting of lots of kinks. The interaction of atoms or molecules with the terrace is repulsive; however, their interaction with the kink is attractive. Because of this difference between the terrace and kink, atoms are only accommodated at the kink, which results in self-assembly of atoms or molecules. If the atomic interaction with the terrace should be attractive also, there would be no atomic self-assembly, resulting in random packing of atoms and the growing film would become amorphous.

In this paradigm of thin film growth, the maximum supersaturation, which would define the maximum growth rate, would be the one which triggers the onset of gas phase nucleation. However, according to Hwang and Lee [6] , the supersaturation that triggers the gas phase nucleation turns out to be so low that the film growth rate without gas phase nucleation is negligibly low and such processing conditions would be hardly adopted in

the thin film industry. In other words, under the process conditions of commercially available thin films the gas phase nucleation occurs in general. This means that thin films are growing inevitably under the condition of gas phase nucleation in most CVD and PVD processes.

It was believed that the gas phase nucleation would be harmful to the thin film growth. Gas phase generated nanoparticles may cause killer defects, resulting in device failure, due to small feature sizes, which are decreasing to < 100 nm [22]. However, Hwang and Lee [10] suggested that the deposition behavior of gas phase generated nanoparticles differs drastically depending on whether they are electrically charged or not. Neutral nanoparticles produce a porous skeletal structure, usually degrading the property of films. However, CNPs tend to be liquid-like and to deposit epitaxially, leaving no voids behind, producing the dense films. The film microstructures evolved by the deposition of CNPs would be difficult to distinguish from those by the deposition of individual atoms or molecules.

Therefore, in order to grow a high quality film at a high deposition rate, it would be necessary to utilize the generation of CNPs in the gas phase. In accordance with this new understanding, Yoshida et al. could grow high T_c super conducting ($YBa_2Cu_3O_{7-x}$) films epitaxially at a rate as highas 16 nm/s by supplying the $YBa_2Cu_3O_{7-x}$ particles using the

plasma flash evaporation method. Cabarrocas [23, 24], Vladimirov and Ostrikov [25],and Nunomura et al. [26] also utilize the incorporation of gas phase nucleated nanoparticles in the plasma enhanced CVD (PECVD) process. During the deposition of silicon by PECVD, Cabarrocas [23, 24] deposited polymorphous films, where gas phase generated crystalline silicon nanoparticles are incorporated into the films. The polymorphous films have better stability and electrical properties than those of amorphous films.

The crystal growth mechanism by the building block of nanoparticles has a long history. For example, more than 40 years ago, Glasner et al.[27-30] suggested that nanometer sized nuclei were generated in the solution with Pb^{2+} during the growth of KBr and KCl. They confirmed that the crystal was grown by self-assembly of the block nuclei in the solution. The crystallinity increased with decreasing size of nuclei. Sunagawa [31, 32], made a similar suggestion that the growth unit of synthetic diamond is not an atom but a much larger unit. These suggestions were not accepted in the crystal growth community largely because the experimental tools were not available at that time to confirm the generation of nanoparticles in solution or in the gas phase. Besides, it was believed that the crystal growth by the building block of nanoparticles would produce aggregates of nanoparticles instead of dense structures. For example, Glasner et al. [27-30]'s suggestion was severely criticized [31] and has been neglected in the crystal growth community.

2. Purpose of this study

Silicon thin film is very useful material for the electrical application such as thin film transistors (TFTs) and thin film solar cells [32, 33]. There are three kinds of silicon films from the viewpoint of microstructure: hydrogenated amorphous silicon (a-Si:H), hydrogenated microcrystalline silicon (μc-Si:H), and crystalline silicon thin film. These type of silicon thin film generally deposited by PECVD or HWCVD using various substrate. When it fabricated at low temperature, it is hard to obtain the high quality epitaxial silicon thin films. Because, diffusivity of silicon atom is very low at that temperature. By the reason, epitaxial silicon thin films are less applied in the industry than amorphous or microcrystalline silicon films.

In general, a-Si:H and μc-Si:H thin films have been used for the active layer of TFTs-liquid crystal display (TFTs-LCD) and for the absorption layer of silicon thin film solar cells. Recently, however, silicon based electric devices need for higher efficiency and performance. Silicon thn film solar cells which have a-Si:H absorption layer gradually decrease its efficiency because of thermal degradation of absorption layer. This well-known phenomena called 'Staebler-Wronski effect' [34]. For this reason, silicon thin film solar cells fabricated tandem structure solar cells in relatively complicate. To obtain higher

and stable efficiency through simple manufacturing process, it is necessary to develop one-step fabrication method of crystalline silicon thin films. In case of active matrix organic light-emitting diode (AMOLED), crystalline silicon films are the key component for advanced performance because AMOLED is current operated device different from voltage operated TFTs-LCD. In summary, Deposition of high quality crystalline silicon films at the low temperature is the ultimate goal for high performance of silicon based electric devices.

The main idea of this study is researching of deposition of epitaxial silicon films by controlling the deposition behaviour of CNPs generated in the gas phase during CVD reactor. From this, it could be possible to deposit high quality epitaxial silicon thin films at the low temperature. Moreover, it could be possible to show the characterization of CNPs and propose the roles of CNPs for the new processing parameter during CVD reactor. These result will be the one of the most important evidence for 'Theory of charged nanoparticles' based on the 'non-classical crystallization'.

Part 2. Chemical vapor deposition for silicon thin films

1. Radio frequency plasma enhanced chemical vapor deposition

Plasma-enhanced chemical vapor deposition (PECVD) is a process used to deposit thin films from a gas state to a solid state on a substrate. Chemical reactions are involved in the process, which occur after creation of a plasma of the reacting gases. The plasma is generally created by RF (AC) frequency or DC discharge between two electrodes, the space between which is filled with the reacting gases. A simple direct-current (DC) discharge can be readily created at a few torr between two conductive electrodes, and may be suitable for deposition of conductive materials. However, insulating films will quickly extinguish this discharge as they are deposited. It is common to excite a capacitive discharge by applying an alternating-current (AC) or radio-frequency (RF) signal between an electrode and the conductive walls of a reactor chamber, or between two cylindrical conductive electrodes facing one another. High-frequency plasmas are often excited at the standard 13.56 MHz frequency widely available for industrial use; at high frequencies, the displacement current from sheath movement and scattering from the sheath assist in

ionization, and thus lower voltages are sufficient to achieve higher plasma densities. This system is called radio frequency plasma enhanced chemical vapor deposition (RF-PECVD).

Fig. 2 shows the RF-PECVD equipment using in this study. The length and width of reaction chamber are 40 cm and 35 cm, respectively. The load lock chamber which has length of 15 cm and width of 18 cm size connected with reaction chamber to insert samples without venting.

The plasma power range of reactor is 10 ~ 250 W and the substrate temperature range of reactor is RT ~ 600 ℃. The flow rates of each precursor and gas were controlled by a mass flow controller (MFC, Tylan). Pure silane (SiH_4 99.9999%, Wonik materials), hydrogen (H_2, 99.9999%, Deokyang energen), and Argon (Ar ,99.999 %, Daesung industrial gases) gases were used as a precursor for deposition of silicon thin films.

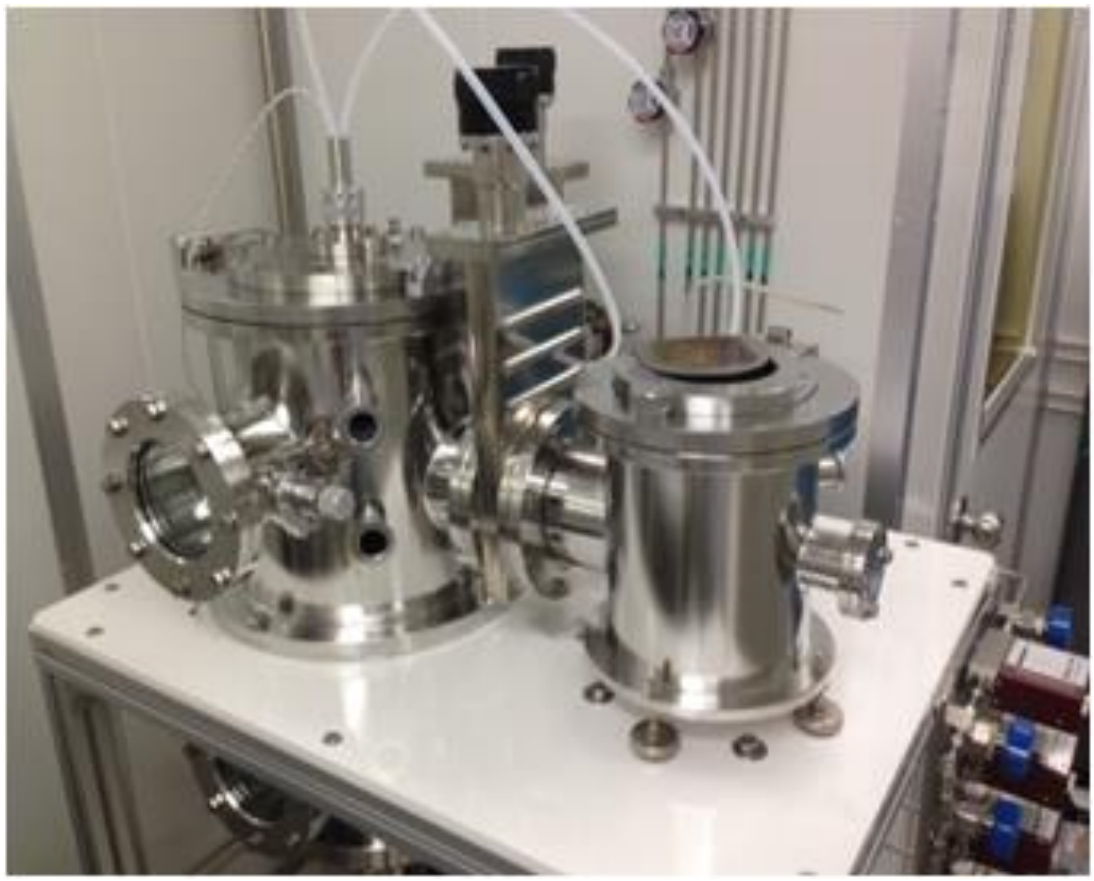

Fig.2. RF-PECVD systems in this study.

2. Hot wire chemical vapor deposition

Hot wire chemical vapor deposition (HWCVD) is a unique deposition technique that involves thermal decomposition of precursor gases at tha surface of resistively heated metal filament. It is also called as catalytic CVD (CAT-CVD) due to the catalytic decomposition mechanism by hot wire.

HWCVD was first introduced in 1979 as ‘thermal CVD’ by Wiesmann et al. [35]. In the 1980s, HWCVD was considered as a new method for the preparation of high quality hydrogenated amorphous silicon with high deposition rate by Doyle et al.[36] and Matsumura et al. [37]. In 1990s, Mahan et al. [38] first report that the device quality hydrogenated amorphous silicon. Since then HWCVD widely investigated for the application of silicon thin film area such as thin film transistors and thin film silicon solar cells.

HWCVD has attracted many researcher’s interest for many decades because it has many advantages. First of all, it could deposit amorphous and microcrystalline silicon films with considerably higher growth rate that of generally used RF PECVD [39].

Fig .3 shows the HWCVD equipment using in this study. The length and width of reaction

chamber is 40 cm and 45 cm. The load lock chamber which has length of 15 cm and width of 20 cm size connected with reaction chamber to insert samples without venting. A showerhead with diameter of 22 cm was placed upper side of reaction chamber for the continuous uniform supply of precursors. The flow rates of each precursor and gas were controlled by a mass flow controller (MFC, Tylan). Hydrogen diluted 30 vol% silane (SiH_4 99.9999 %, Wonik materials) ,5 vol% phosphine (PH_3 99.9999%, Air liquid), and 5 vol % diborane (B_2H_6 ,99.9999%, Air liquid) gases were used as precursors. For the epitaxial silicon films, appropriate amount of the HCl gas (99.999 %, Tsurumi Soda) was supplied additionally. The substrate temperature range of reactor is RT ~ 600℃.

Fig.3. HWCVD systems in this study.

Chapter 2. Low temperature deposition of epitaxial silicon thin films during RF-CVD

Part 1. Introduction

1. Background and purpose of this study

Silicon thin films have been extensively used in electrical devices for thin film transistor (TFTs) and silicon thin film based solar cells [40-43]. But when it fabricated at low temperature, it is hard to obtain the high quality epitaxial silicon thin films. Because, the diffusivity of silicon atom is very low at that temperature. By the reason, epitaxial silicon thin films are less applied in the industry than amorphous or microcrystalline silicon films.

Until now, deposition of nanostructure or films explained by classical crystallization based on atomic or molecules growth [20, 21, 44]. However, there have been experimental results, which cannot be properly explained by this classical crystallization [8, 45]. Rather such experimental results imply that nanostructure or films should be grown by the growth unit of nanoparticles, whose way of crystal growth is called ‘non-classical crystallization’ [1-5], Hwang et al.[8-11] studied extensively the non-classical crystallization in the chemical vapor deposition (CVD) process.

They suggested that the electrically charged nanoparticles (CNPs) were the grow units of

nanostructures and films and the electric charge played a critical role. This is why they called this new growth mechanism in the gas phase synthesis ‘theory of charged nanoparticles (TCN)’. According to this theory, CNPs are spontaneously generated in the gas phase in most CVD processes. TCN was first suggested to explain the paradoxical experimental observation of simultaneous deposition of less stable diamond and etching of stable graphite. This phenomenon violates the second law of thermodynamics if approached by the classical concept of crystal growth by an atomic unit. But the TCN could successfully explain the paradoxical experimental observation [8]. The TCN could also explain the puzzling phenomena that a diamond film deposits on a silicon substrate whereas a porous skeletal soot structure deposits on an iron substrate under the same processing condition [45]. The generation of CNPs, which was predicted to form in the gas phase during CVD was experimentally confirmed not only in the Si CVD process [46-49] but also in many other CVD processes [13, 16, 18, 50]. Also utilize the incorporation of gas phase nucleated nanoparticles in the plasma enhanced CVD (PECVD) process. During the deposition of silicon by PECVD, Cabarrocas [24, 51-53] deposited polymorphous films, where gas phase generated crystalline silicon nanoparticles are incorporated into the films. The polymorphous films have better stability and electrical properties than those of amorphous films.

If nanoparticles are neutral, they undergo random Brownian coagulation, and they are difficult to accommodate the crystal structure of substrate. If they are charged, however, they are easy to accommodate the crystal structure of substrate. This is attributed to the property of CNPs, which are liquid-like. Hwang et al. [6, 7] suggested that nanoparticles with a large amount of charge are more liquid-like than nanoparticles with a small amount of charge. This suggestion based on the bonding strength of nanoparticles might be weakened by the presence of charge. Clare et al. [54]showed that the charge weakens the bond strength by the abinitio study of the charge effect on the bond strength.

2. Charged enhanced diffusion

The effect of a single negative or positive charge on the strength of silicon-silicon and silicon-hydrogen bonds in the molecules SiH_4 and Si_2H_2 was calculated by ab initio calculations. To determine the difference in the energy to break a single Si-H bond in SiH_4, SiH_4^+, and SiH_4^-, calculations were done on six species: SiH_3, SiH_4, SiH_3^-, SiH_4^-, SiH_3^+, and SiH_4^+ and the required energies were determined by comparing the bond strength of each species. Similar calculations were done with the species Si_2H_6, Si_2H_5, $Si_2H_6^-$, $Si_2H_5^-$, $Si_2H_6^+$, and $Si_2H_5^+$ to observe the effect of a lower charge/size ratio and to examine the

effect of charge on the Si-Si bond energy. The results of ab initio calculations are shown in Table 1.

When the atoms are embedded in a lattice, they will not be free to attain geometries resembling the optimized ion geometry although they will be able to relax to some degree. Thus the actual effects of charge on bond strength in hydrogenated amorphous silicon will be between those indicated by the unoptimized (adiabatic) and optimized (vertical) rows of Table 1. They are likely to be closer to those for the unoptimized rows.

Both positive and negative charges drastically weaken the bond strength of Si-Si and Si-H. The bond strength of Si-Si is weakened from 3.2 eV to 1.11 eV when Si_2H_6 is negatively charged. It is weakened to 1.6eV when Si_2H_6 is positively charged. The bond strength of Si-H is weakend more drastically from 3.9 eV to 0.98 eV when SiH_4 is negatively charged. It is weakened to 0.3 eV when SiH_4 is positively charged.

The effect of charge on the bond strength can be explained by bond order. A bond order, which represents the strength or stability of bond, is the number of bonding electron pairs shared by two atoms in a molecule. In the molecular orbital theory, a bond order is defined as half the difference between the number of bonding electrons and the number of antibonding electrons as expressed by the following equation,

$$\textbf{Bond order} = \frac{\#\ of\ bonding\ electrons - \#\ of\ antibonding\ electrons}{2} \quad (1)$$

If a cluster is charged negatively, electrons are added to the antibonding orbital. If a cluster is charged positively, electrons are removed from the bonding orbital. Therefore both positive and negative charges would decrease the bond order and thereby weaken the bond strength.

Weakening of bond strength by charge has very important implications because it means that diffusion or kinetics is enhanced. The new concept of charge-enhanced diffusion can explain the liquid-like property of CNPs, which was suggested by Hwang et al.[7]. This concept can also explain the rapid kinetics of coalescence in Figures 2 and 3. The concept of charge-enhanced kinetics can explain the enhanced chemical reactions of reactant gases even at low temperature in the PECVD process. It also explains the deposition of crystalline films at low temperature.

Moreover, there are many processes where ion or electron beams are used to enhance the kinetics at low temperature. For example, high quality films can be grown at low temperature by ion-beam assisted deposition (IBAD) in the sputtering or evaporation

processes. Also there is a process called gas-mediated electron or ion beam induced deposition and etching, where beams of electrons and ions are used to modify a surface locally at micron and submicron dimensions or fabricating in three dimensions [42-44]. In all these process, the enhanced kinetics is not clearly understood, vaguely explained by the bombarding energy of ions or electrons. However, it is highly probable that the enhanced kinetics should come from weakening of the bond strength by charge. Moreover, the effect of charge on weakening the bond strength and thereby enhancing the kinetics seems to be very general, even related with the catalytic effect and the enzyme activity in biology.

Zheng et al. [55]observed the superplastic deformation behaviour of nanoscale amorphous silica near room temperature using in situ experiments inside a TEM with low beam intensities without obvious rise in sample temperature. They called the phenomenon electron-assisted superplasticity. After imaging for the positioning of the sample and the diamond flat punch, the beam was blocked off with the condenser lens aperture, and the silica particle was compressed with the Hysitron Pico-indenter [56]. The particle is plastically deformed because of the e-beam irradiation it had experienced during the imaging. After ~ 40 percent compression [57], where the contact pressure is estimated to be 9.2 GPa, the beam was brought on the sample to image the particle. On un-loading, the total plastic percent compression was 27%. On compressive loading again with beam on,

surprisingly, the plastic flow of the glass was continuous and smooth, with no sign of shear banding or cracking. Much easier flow was observed, with the ensuing beam-on deformation in a second set of in situ experiments, resulting in a pancake shape. Although the contact area kept increasing, the forces required to deform were at levels considerably lower than those in the beam-off condition. This phenomenon of electron-assisted super plasticity might also be explained by weakening of bond strength by charge.

Compound	Si—H (eV)	Si—Si (eV)
SiH_4 (optimized)	3.9	—
SiH_4^- (optimized)	0.98	—
SiH_4^+ (optimized)	0.30	—
Si_2H_6 (optimized)	3.5	3.2
$Si_2H_6^-$ (optimized)	1.02	1.11
$Si_2H_6^+$ (optimized)	1.59	1.6
SiH_4^- (unoptimized)	1.35	—
SiH_4^+ (unoptimized)	0.09	—
$Si_2H_6^-$ (unoptimized)	1.34	1.3
$Si_2H_6^+$ (unoptimized)	1.49	1.6

Table. 1 Calculated bond strengths of Si-H and Si-Si. [54].

Part .2. Experimental confirmation of behavior of charged nanoparticles during RE-PECVD by capturing the particles

1. Experimental details

Silicon thin films were deposited using an RF-PECVD reactor with separate bias supply system. The substrate temperature was controlled with a self-regulating heating system and the temperature of substrate was measured by the direct contact of a thermocouple with the substrate. The plasma power was fixed at 125 W and the reactor pressure was fixed at 1 torr. The flow rates of each precursor and gas were controlled by a mass flow controller (MFC, Tylan). Pure silane (SiH_4 99.9999 %, Wonik materials), hydrogen (H_2, 99.9999 %, Deokyang energen), and Argon (Ar, 99.999 %, Daesung industrial gases) gases were used as a precursor for deposition of silicon thin films. The flow rates of SiH_4, H_2, and Ar were fixed at 2 standard cubic centimeters per minute (sccm), 48 sccm, and 10 sccm, respectively.

To observe the initial silicon nanoparticles formed in the gas phase varied with the substrate bias, the silicon nanoparticles were captured on Cu grids with silicon monoxide and carbon membranes for 15 sec using a shutter covering the grid membrane. To confirm the effect of substrate conductivity, particles were captured on two difference membranes, which were insulating silicon monoxide membrane and conducting carbon membrane. The biases were applied to the substrate at the biases of 0 V, +1000 V, -1000 V, respectively. The grids were observed by high resolution transmission electron microscope (HRTEM, F30, FEI) operated at 200 KeV.

2. Result and discussion

Fig.4 shows the silicon nanoparticles captured for 15 sec on the insulating silicon monoxide membrane of the Cu grid with substrate bias. There was not quite difference in size and amount of particles between Fig. 4(a)-(c). However, the dispersion of the particles was different in each condition. In Fig. 4(a) and (b), silicon nanoparticles were relatively well dispersed on the silicon monoxide membrane. On the other hand, Fig. 4(c) shows that the silicon nanoparticles were gathered in the center of the silicon monoxide membrane. This means that the particles were deposited freely on the silicon monoxide membrane at

the condition of non-bias or positive bias. But, at the negative bias condition, the particles were influenced by the electrostatic force which gathered particles in the center of silicon monoxide membrane and a depletion zone was appeared.

Fig.5 shows that the HRTEM images of silicon nanoparticles in the Fig.4. In Fig. 5(a), which is HRTEM image of particles captured without substrate bias, it is hard to find the crystalline particles.

In Fig. 5(b), which is HRTEM image of particles captured with 1000 V substrate bias, the crystalline phase was present in some proportion. In Fig.5(c), particles, which were captured with -1000 V substrate bias, had a large amount of crystalline phase.

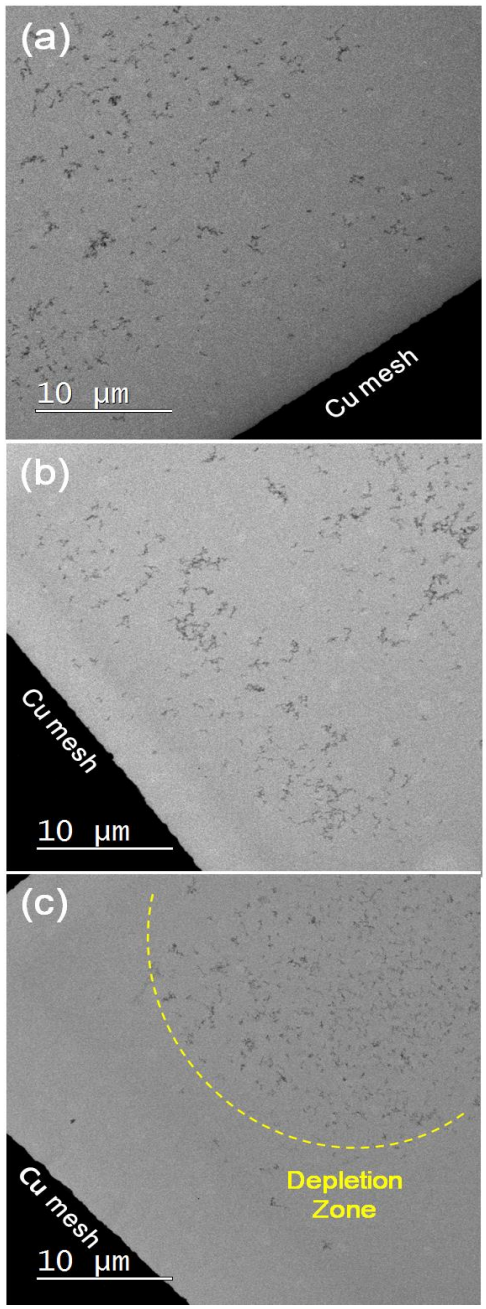

Fig.4. TEM images of silicon nanoparticles captured on SiO TEM grid with an exposure time of 15 sec for (a) 0 V, (b) +1000 V, and (c) -1000 V.

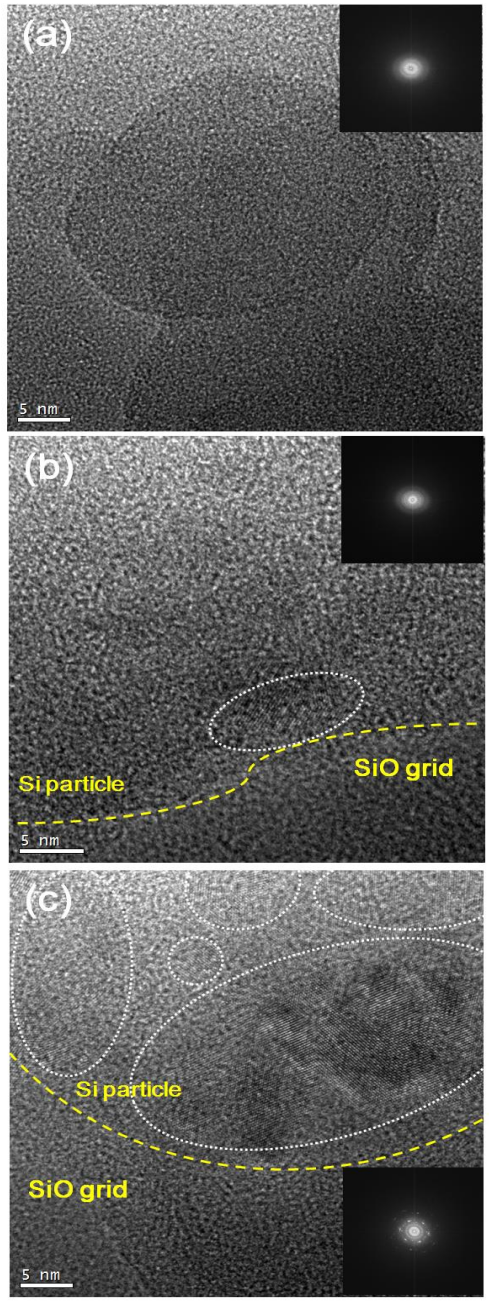

Fig.5. HRTEM images of silicon nanoparticles captured on SiO TEM grid with an exposure time of 15 sec for (a) 0 V, (b) +1000 V, and (c) -1000 V.

Fig.6 shows the silicon nanoparticles captured for 15 sec on the conducting carbon membrane of the Cu grid with substrate bias for 0 V, +1000 V, and –1000 V respectively. Even other deposition conditions were same as those of Fig.4, the capture behaviors on the conducting carbon membrane were quite different from those of insulating silicon monoxide membrane. As same with previous results in Fig.4, there is no difference in size and amount of particles between Fig. 6(a)-(c). However, the amount of particles was increase than that of Fig.4. Also all the nanoparticles in Fig.6 were well dispersed on the conducting carbon membrane. The dispersion of particles was independent of substrate bias.

Fig.7 shows that the HRTEM image of silicon nanoparticles in the Fig. 6. In Fig. 7(a), which is HRTEM image of particles captured without substrate bias, it is hard to find the crystalline phase in the particles. In Fig.7(b) and (c), which are HRTEM images of particles captured with substrate bias +1000 V and -1000 V, particles had a large amount of crystalline phase.

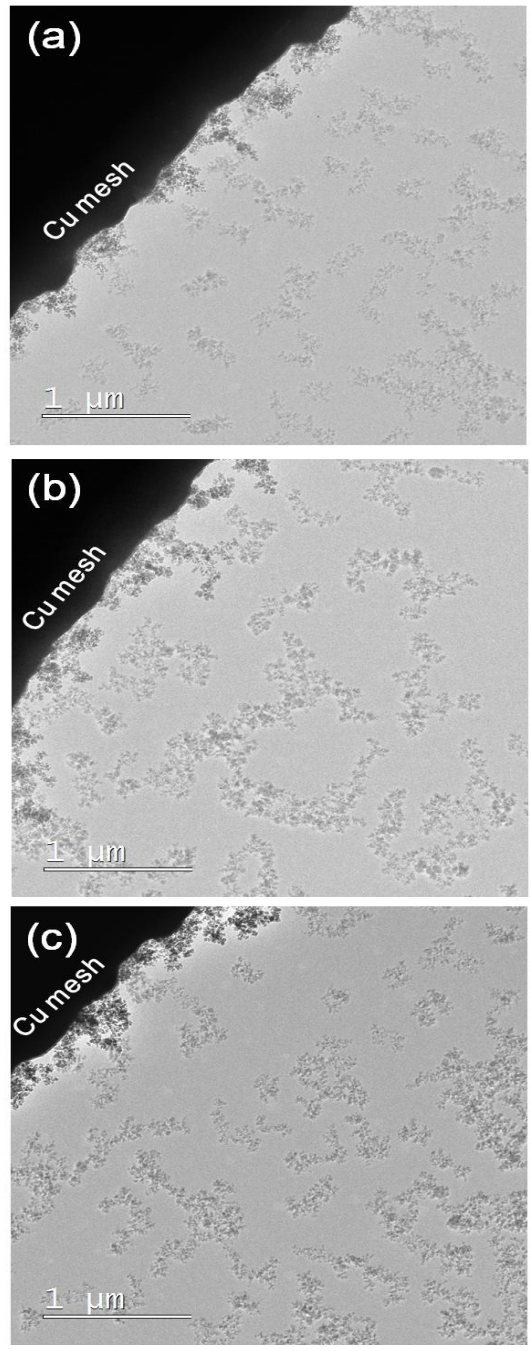

Fig.6. TEM images of silicon nanoparticles captured on carbon TEM grid with an exposure time of 15 sec for (a) 0 V, (b) +1000 V, and (c) -1000 V.

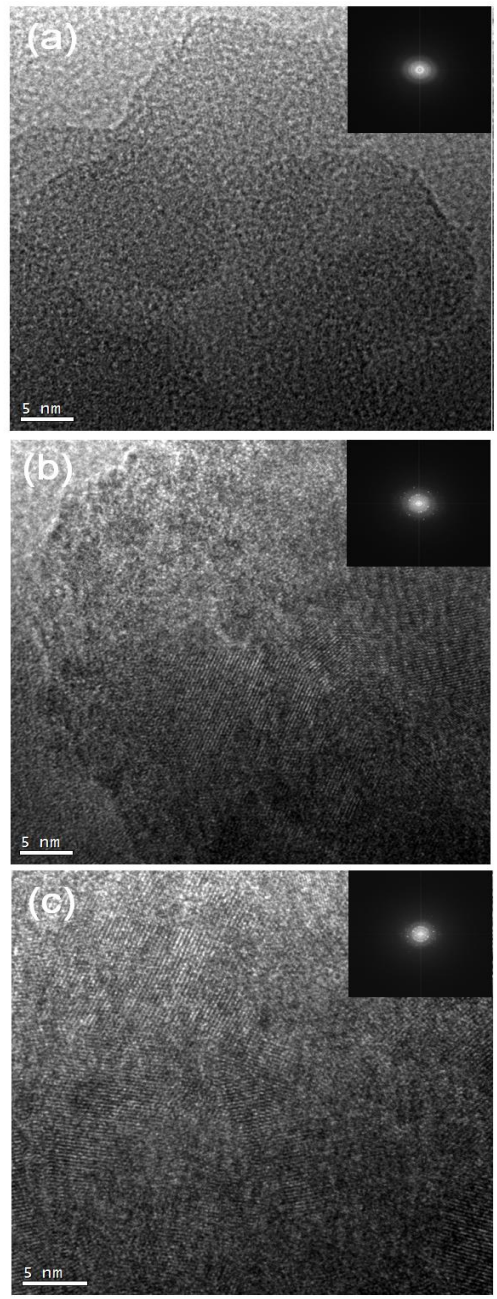

Fig.7. HRTEM images of silicon nanoparticles captured on carbon TEM grid with an exposure time of 15 sec for (a) 0 V, (b) +1000 V, and (c) -1000 V.

The behavior of captured nanoparticles on the TEM grid in Figs. 4-7 is the puzzling phenomenon. But it could be explained by TCN. If nanoparticles generated in the gas phases were charged, they would be affected by the substrate biases. It means that in the condition with positive bias, negatively CNPs are selectively deposited and in the condition with negative bias, positively CNPs are selectively deposited. If particles are captured in the condition without bias, both CNPs and neutral particles would be randomly deposited. If applying a bias to the substrate, in case of positive bias, electrons would be preferentially attracted to the grid and in case of negative bias, ion would be preferentially attracted to the grid. In this case, charge could not be accumulated on the conducting Cu mesh. But, if membrane, such as silicon monoxide, is insulating, charge would be accumulated on the membrane. Also, in general, the particles are more attracted to a conducting materials than an insulating materials [58]. Therefore, the CNPs are more attracted toward the Cu mesh than membrane by the electric force. Therefore, the amount of charge of particles is significant issue in the behavior of captured nanoparticles. If the particles with a small amount of charge and neutral particles are captured on the grid, they would be relatively uniformly deposited due to weak electric force which was shown in fig. 4(a) and (b). On the other hand, the multiply charged particles are captured on the grid, they were strongly attracted towards the mesh, the particles which near the mesh was

captured on the mesh. In that reason, nanoparticles were gathered in the center of the silicon monoxide membrane and the depletion zone was appeared which was shown in fig. 4(c). If both the mesh and membrane is conducting, this tendency was disappeared. These results can be confirmed in Fig. 6. From these results, we could confirm that the CNPs are the growth units of silicon film deposition, and positively CNPs which were captured by negative substrate bias are more charged than negatively CNPs which were captured by positive substrate bias.

Fig. 5 and 7 shows that the crystalline phase proportion of captured particles was varied depending on the substrate bias. In the condition without bias, amorphous particles were mostly captured. However, with bias, captured particles had a large amount of crystalline phase. The results show that the CNPs which were selectively captured on the membrane by substrate bias had higher crystalline proportion than that of neutral nanoparticles. Therefore, the CNPs, which were selectively captured on the membrane by substrate, were advantageous for the epitaxial film growth.

3. **Conclusion**

TEM observation of silicon CNPS shows that the behavior of CNPs depends on the substrate bias and the conductivity of substrate. As a result, we confirmed that the nanoparticles generated in the RE-PECVD reactor are charged and we also could confirm that the CNPs are the growth units of silicon film deposition, and positively CNPs which were captured by negative substrate bias are more charged than negatively CNPs which were captured by positive substrate bias.

Part. 3. Homo-epitaxial growth of silicon films during RF-PECVD

1. Experimental details

Silicon thin films were deposited using an RF-PECVD reactor with separate bias supply system. The substrate temperature was controlled with a self-regulating heating system and the temperature of substrate was measured by the direct contact of a thermocouple with the substrate. The plasma power was fixed at 125 W and the reactor pressure was fixed at 1 torr. The flow rates of each precursor and gas were controlled by a mass flow controller (MFC, Tylan). Pure silane (SiH_4 99.9999 %, Wonik materials), hydrogen (H_2, 99.9999 %, Deokyang energen), and Argon (Ar, 99.999 %, Daesung industrial gases) gases were used as a precursor for deposition of silicon thin films. The flow rates of SiH_4, H_2, and Ar were fixed at 2 standard cubic centimeters per minute (sccm), 48 sccm, and 10 sccm, respectively.

To measure thickness of the silicon film varied with the substrates and bias by deposition

time, silicon thin films were deposited on the 1 cm × 1 cm Corning Eagle XG glass, p-type (100) silicon wafer and Fe-3 wt% steel substrates. The substrate temperature was fixed at 400 ℃ and the deposition time were 3, 5, 10, 15 minutes, respectively. The thickness of films was measured by the surface profile of Alpha-Step IQ (Rev. AL-1).

To examine effect of bias in deposition of homo-epitaxial silicon films, silicon films were deposited on the 1 cm × 1 cm p-type (100) silicon wafers at 550 ℃. The substrate biases were applied to 0 V, +1000 V, -1000 V, respectively. For epitaxial growth, the silicon wafers were pretreated by dipping in a 5 % HF solution in order to remove an organic residues and a native oxide. To observe the cross sectional microstructure of the silicon films, TEM specimens were prepared using a focused ion beam (FIB, Nova 200, FEI). The specimens were observed by high resolution transmission electron microscope (HRTEM, F30, FEI) operated at 200 KeV.

2. Result and discussion

Fig. 8 shows the deposition rate of silicon films deposited various substrates and

substrate bias. Glass, silicon wafer, and Fe were used as substrates and the bias was applied to the substrate at the biases of 0 V, +1000 V, -1000 V, respectively. Fig. 8(a) shows that the deposition rate of silicon film up to 15 min. with 0 V, +1000 V, -1000 V biases. On the glass and silicon wafer, the deposition rate of the condition with bias is comparable to that of the condition with non-bias. In the Fe substrate, however, the deposition rate of the condition with bias is higher than to that of the condition with non-bias. Fig. 8(b)-(c) shows the deposition rate with deposition time in various substrates. Fig. 8(b) presents the deposition rate with deposition time in the glass substrate. The deposition rate without bias condition was relatively uniform over time. On the other hand, the deposition rate with bias condition was high in the early time of deposition but decreased with time. Even, at the early time of deposition, the deposition rate of the condition with bias is higher than to that of the condition with non-bia, the difference of deposition rate between the condition with bias and without bias decreased gradually over time. It tends to be saturated after a deposition time of 15 min. Fig. 8(c) shows the deposition rate with deposition time in the silicon wafer substrate. The tendency of the deposition rate variation was similar to that of the glass substrate. But the difference of deposition rate between the early and late deposition time was reduced. Fig. 8(d) shows the deposition rate with deposition time in the Fe substrate. Even the tendency of the

deposition rate variation was similar to that of the glass and silicon wafer substrate, the difference of deposition rate between the condition with bias and without bias is bigger than that of glass and silicon wafer substrates.

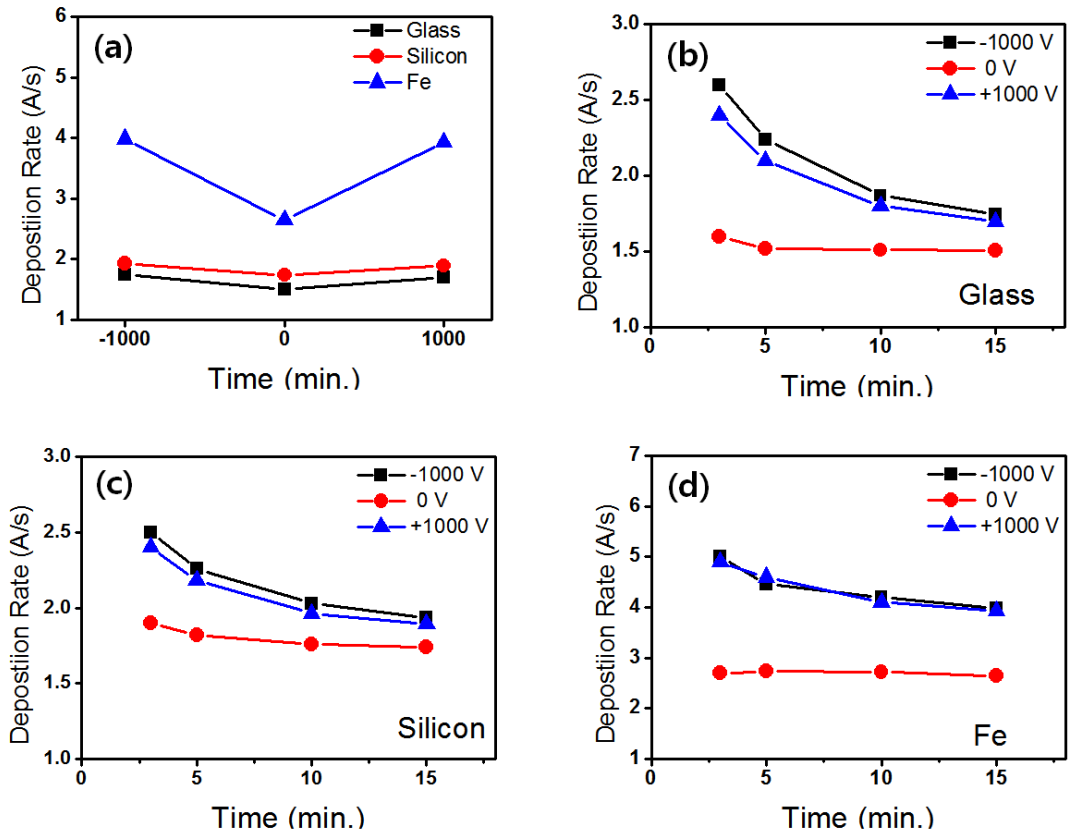

Fig.8. The growth rate of silicon films prepared with varying substrates and bias. (a) The growth rate of silicon films deposited for 15 min. with varying substrates. (b) The growth rate of silicon films on the glass substrate at various time, (c) The growth rate of silicon films on the silicon wafer at various time intervals, (d) The growth rate of silicon films on the Fe substrate at various time intervals.

Fig. 9 shows TEM images of the silicon film deposited on a silicon wafer by the deposition condition without bias. Fig. 9(a) shows an overall cross section image of the film. This image consists of two layers distinguished by the contrast. The lower grey layer is the silicon wafer with the upper white layer being the deposited silicon film. Fig. 9(b) shows a magnified image of the interfacial layers, which are indicated by the square in Fig. 9(a). The dark gray columnar structure was observed partially in the deposited silicon film. This microstructure of film was common in the silicon film deposition [59, 60]. Fig. 9(c) shows a HRTEM image of the interfacial region, which are indicated by the square in Fig. 9(b). In columnar structure, poly crystalline silicon phase was deposited. Outside of the columnar structure, microcrystalline silicon, which has small grains of crystalline silicon within the amorphous phase, was deposited. However, Epitaxial growth was not occurred at all.

Fig. 10 shows TEM images of the silicon film deposited on a silicon wafer by the deposition condition with +1000 V bias. Fig. 10(a) shows an overall cross section image of the film. This image consists of three layers which are silicon wafer layer, epitaxial layer, and microcrystalline layer. The dark gray inverted columnar structure was observed near the interface between the silicon wafer and the deposited film. Fig. 10(b) shows HRTEM image of the middle of the film, which are indicated by the square in Fig. 10(a). Right dark

gray layer is part of the inverted columnar structure, which was described in Fig. 10(a). left gray layer is part of the microcrystalline layer. Fig. 10(b) shows that the inverted columnar structure was composed of a single crystal structure. Fig. 10(c) shows that a HRTEM image of the interfacial region, which are indicated by the square in Fig. 10(a). Fig. 10(c) indicated that epitaxial growth was occurred in the form of an inverted columnar structure near the interface. However, the epitaxial growth breaks down abruptly and the microstructure changes to the microcrystalline silicon as shown in Fig. 10(a) and (b).

Fig. 11 shows TEM images of the silicon film deposited on a silicon wafer by the deposition condition with -1000 V bias. Fig 11(a) shows an overall cross section image of the film. This image consists of two layers. The lower layer is the silicon wafer with the upper layer being the deposited silicon film. HRTEM images of the upper and the interfacial layers, which are indicated by the square in Fig. 11(a), are shown respectively in Figs. 11(b) and 11(c). Fig. 11(b) shows HRTEM image of the middle of the film, which are indicated by the square in Fig. 11(a). Fig. 11(b) and (c) shows that the fully homo-epitaxial silicon film was deposited in condition with -1000 V. on the silicon wafer. There are no breaks down of epitaxial growth or the microcrystalline silicon phase.

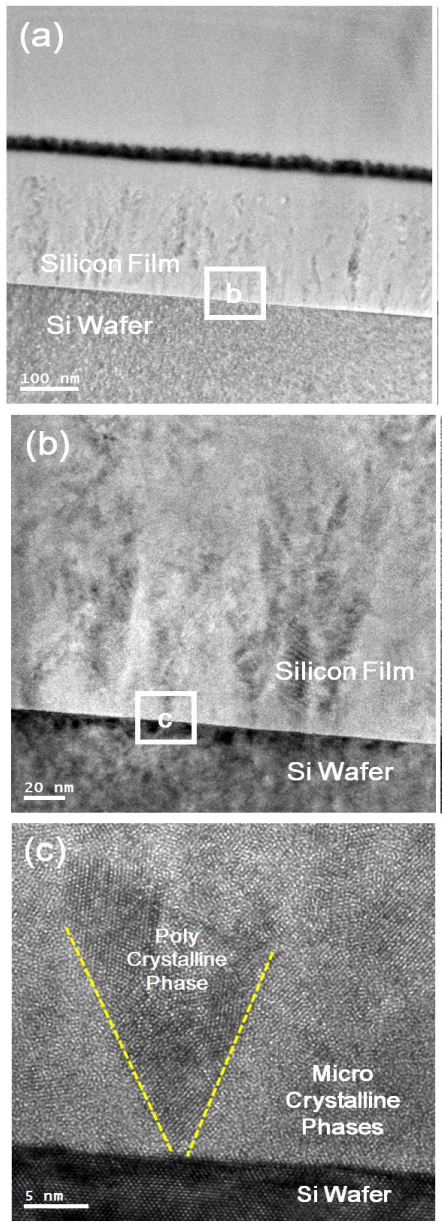

Fig.9. TEM cross section images of the silicon films on (100) silicon wafer with 0 V. (a) low magnification TEM image of films, (b) TEM image of the silicon of the interfacial region between silicon wafer and silicon film, and (c) HRTEM image of the interfacial region.

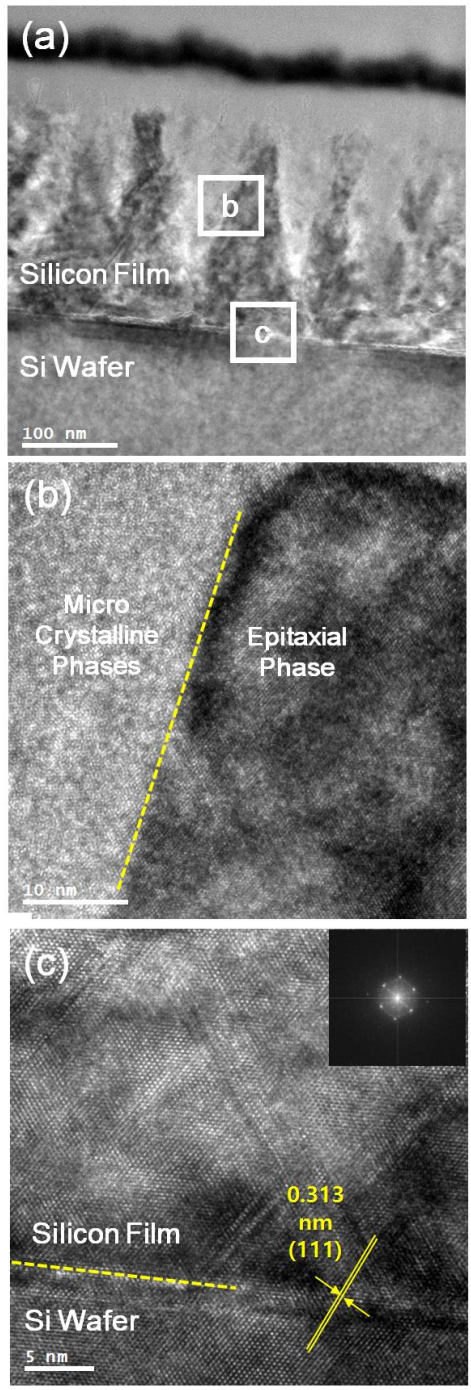

Fig.10. TEM cross section images of the silicon films on (100) silicon wafer with 1000 V. (a) low magnification TEM image of films, (b) HRTEM image of the silicon film at middle part, and (c) HRTEM image of the interfacial region between silicon wafer and silicon film.

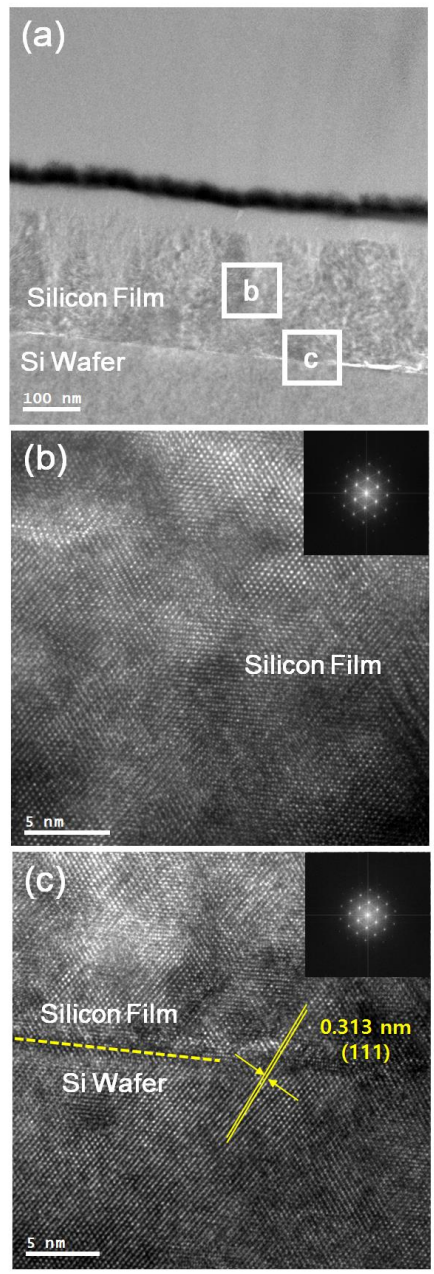

Fig.11. TEM cross section images of the silicon films on (100) silicon wafer with -1000 V. (a) low magnification TEM image of films, (b) HRTEM image of the silicon film at middle part, and (c) HRTEM image of the interfacial region between silicon wafer and silicon film.

If the growth unit of deposition is CNPs, the deposition rate of films might be modified by substrate bias. Therefore, the difference of deposition rate by the substrate bias in Fig. 5 is significant evidence of TCN. If the growth units of deposition is neutral, the difference of deposition rate could not be occurred. But the growth units of deposition, which are CNPs, are charged, the deposition rates differ by the substrate bias. However, in fig. 5(a), even deposition rate of films on Fe substrate was large differed by the substrate bias, deposition rates of films on glass and silicon wafer substrates were small differed by the substrate bias. These phenomenon could be explained by the difference of the deposition rate over time in Fig. 5 (b)-(d).

As mentioned earlier, in the condition with bias, charge was accumulated on the low conductivity substrate by deposition of one sign particles. In the early time of deposition on low conductivity substrates, such as glass or silicon wafer, the CNPs was accelerated by the substrate bias. Since this acceleration, the deposition rate of films was higher than that of condition without bias. But, in the later time of deposition, the charge was accumulated on the substrate and this accumulated charge prevented the effect of substrate bias, which causes the acceleration of the particles. For this reason, the deposition rate was gradually reduced with deposition time and finally the deposition rate in the condition with bias became similar to that in the condition without bias. Conversely, on the conducting

substrate, however, the charge could not be accumulated on the substrate. Therefore, the substrate bias effect is maintained over deposition time. By this reason, on the conducting substrate, such as Fe, deposition rate in the condition with bias was consistently higher than that in the condition without bias.

According to TCN, the amount of charge of the particles increase, the particles is favor for epitaxial growth by enhancement of diffusion [61]. Therefore, to deposit an excellent epitaxial film, the particles with the large amount of charged were selectively deposited. In the previous results, we could know that positively CNPs which were deposited by negative substrate bias had a large amount of charge. Thus, if the silicon films were deposited in the condition with negative bias, excellent epitaxial films could be deposited. Fig. 6-8 shows that the TEM images of the silicon film deposited on a silicon wafer by the deposition condition with 0V, +1000 V, -1000 V biases.

Without acceleration of particles by bias, epitaxial film was not deposited at all shown in Fig. 6. However, with acceleration of particles by bias, silicon homo-epitaxial film was deposited on the silicon wafer. In the condition with positive bias, negatively charged particles were selectively deposited. However, we confirmed that these negatively charged particles had less amount of charge than positively charged particles in Fig. 1. Thus liquid

like property of these particles was not enough to be deposited epitaxial film. In the later time of deposition, charge was accumulated on the films and effect of bias was weakened, because deposited film was insulating. In that reason, silicon homo-epitaxial film was broken down from the middle of the film. This deposition behavior was shown in Fig. 7. In the condition with negative bias, positively charged particles were selectively deposited. Positively charged particles would be multiply charged and these particles were enough to be deposited fully epitaxial film. Therefore, although charge was accumulated on the films and effect of bias was weakened, fully epitaxial film was deposited in the condition with negative bias. These deposition behavior presents effect of bias during deposition of epitaxial growth.

3. Conclusion

Homo-epitaxial silicon films could be deposited at 550 ℃ by negative substrate bias. The deposition behavior and deposition rates depended on the substrate bias. Multiply CNPs, which were attracted by negative substrate bias, favor the silicon epitaxial films. This deposition behavior of films can be applied to the low temperature epitaxial film growth.

Part. 4. Hetero-epitaxial growth of silicon films during RF-PECVD

1. Experimental details

Silicon thin films were deposited using an RF-PECVD reactor with separate bias supply system. The substrate temperature was controlled with a self-regulating heating system and the temperature of substrate was measured by the direct contact of a thermocouple with the substrate. The plasma power was fixed at 125 W and the reactor pressure was fixed at 1 torr. The flow rates of each precursor and gas were controlled by a mass flow controller (MFC, Tylan). Pure silane (SiH_4 99.9999 %, Wonik materials), hydrogen (H_2, 99.9999 %, Deokyang energen), and Argon (Ar, 99.999 %, Daesung industrial gases) gases were used as a precursor for deposition of silicon thin films.

To examine effect of bias in deposition of Hetero-epitaxial silicon films, silicon films were deposited on the 1 cm × 1 cm n-type (100) germanium wafers at 550 ℃. The substrate

biases were applied to -1000 V, respectively. For epitaxial growth, the silicon wafers were pretreated by dipping in a 5 % HF solution in order to remove an organic residues and a native oxide. To observe the cross sectional microstructure of the silicon films, TEM specimens were prepared using a focused ion beam (FIB, Nova 200, FEI). The specimens were observed by high resolution transmission electron microscope (HRTEM, F30, FEI) operated at 200 KeV.

2. Result and discussion

Fig. 12 shows TEM images of the silicon film deposited on a germanium wafer by the deposition condition with -1000 V bias. The flow rates of SiH_4, H_2, and Ar were fixed at 2 standard cubic centimeters per minute (sccm), 48 sccm, and 10 sccm. Fig. 12(a) shows an interfacial cross section image of the film. This image consists of two layers. The lower layer is the silicon wafer with the upper layer being the deposited silicon film. Fig. 12(b) shows the TEM image of middle parts of film. The silicon film which was deposited in this condition, the microcrystalline silicon film was observed. The epitaxial film, however, could not be deposit at all.

Fig. 13 shows TEM images of the silicon film deposited on a germanium wafer by the deposition condition with -1000 V bias. The flow rates of SiH_4, H_2, and Ar were fixed at 1 standard cubic centimeters per minute (sccm), 49 sccm, and 10 sccm. The silane ratio was reduced by half than that of condition in Fig. 13. Fig. 13(a) shows an interfacial cross section image of the film. This image consists of two layers. The lower layer is the silicon wafer with the upper layer being the deposited silicon film. Fig. 13(b) shows the TEM image of middle parts of film. In this condition, fully hetero epitaxial film was deposited on germanium wafer although there exist some stacking faults. This phenomenon was due to the size of CNPs. According to TCN, if nanoparticles are neutral, they undergo random Brownian coagulation, producing a very porous structure. If they are charged, however, they deposit as dense films, not leaving voids behind. This is attributed to the property of CNPs, which undergo self-assembly and are liquid-like, resulting in epitaxial recrystallization. They suggested that small CNPs are more liquid-like than large ones because the number of atoms per charge increases with increasing size of CNPs for the same amount of charge. The liquid-like property of small CNPs was deduced from the experimental observations that dense crystalline films are produced by the deposition of CNPs whereas porous skeletal structures are produced by the deposition of neutral nanoparticles. Besides, it was also observed that the crystalline quality increases with

decreasing size of CNPs. These results imply that the bonding strength of nanoparticles might be weakened by the presence of charge. Indeed, the abinitio study of the charge effect on the bond strength by Clare et al. [54] showed that the charge weakens the bond strength. Hwang et al. [6] reported that the size of CNPs in the gas phase increased with increasing flow rate of silane in the silicon HWCVD process. In order to enhance the epitaxial growth, the deposition condition should be made in such a way to make CNPs as liquid-like as possible by decreasing their size Therefore, the deposition behavior of CNPs would depend critically on their size as suggested by Jung et al. [7]. To grow an epitaxial film, CNPs should be made as liquid-like as possible. To achieve this condition, the size of CNPs should be minimized by reducing flow rate of silane. For example, the deposition condition of Fig. 13 represented decreased flow rate of reactant gases resulted in successful epitaxial growth.

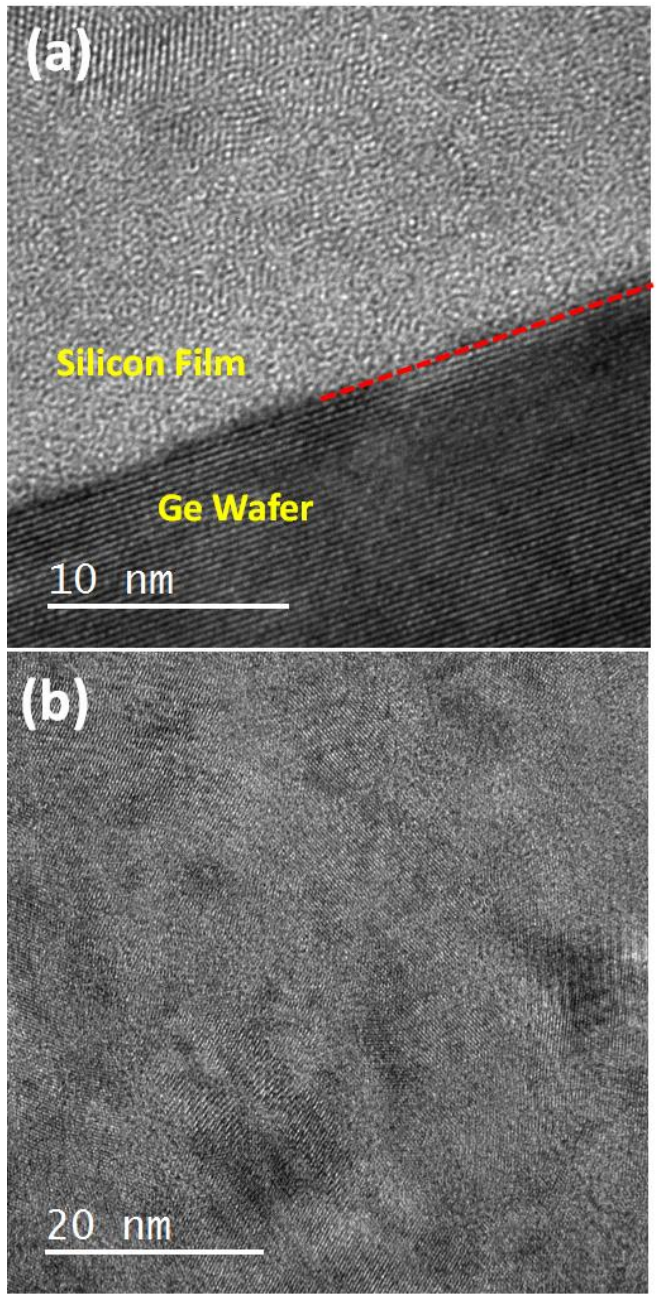

Fig.12. TEM cross section images of the silicon films on (100) Germanium wafer without bias. (a) HRTEM image of the silicon film of the interfacial region between silicon wafer and silicon film, and (c) HRTEM image at middle part of film

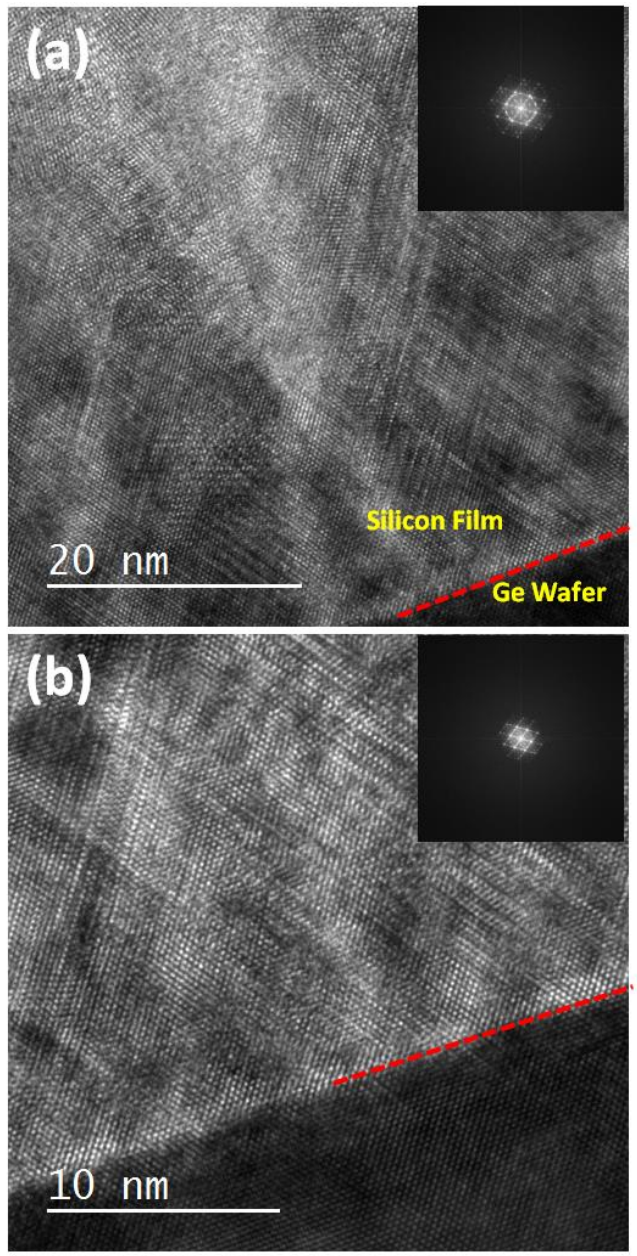

Fig. 13. TEM cross section images of the silicon films on (100) Germanium wafer with -1000 V. (a) HRTEM image of the silicon film of the interfacial region between silicon wafer and silicon film, and (c) HRTEM image at middle part of film

3. Conclusion

The silicon hetro-epitaxial film was deposited on the germanium substrate by reducing flow rate of silane. The deposition behavior depends on the size of these nanoparticles. Small CNPs favor the epitaxial growth. This result represent that the size of CNPs is crucial parameter of deposition of thin film.

Chapter 3. Low temperature deposition of Homo-epitaxial silicon thin films on a silicon wafer during HWCVD

Part. 1. Introduction

1. Background and purpose of this study

The size of CNPs is also a critical factor in the thin film growth by CVD. Therefore the information about the size distribution of CNPs is important in controlling the microstructure evolution of films. The size of nanoparticles increases normally as the concentration of reactant source gases increases. Fig. 14 shows the measured mass distributions of negative CNPs for four different methane concentrations during HWCVD. During the mass distribution measurements, diamonds were deposited in situ on a Mo substrate placed near the orifice with a substrate temperature of 750 ^{o}C. The diamond films deposited at 1% and 1.5% CH_4, where nanoparticles of 200~300 carbon atoms were dominant in Fig. 14, showed good crystalline quality as shown in Fig. 15(a). At the condition for methane concentrations of 3% and 5%, where the nanoparticles in the gas phase contained more than 1000 carbon atoms and the size distribution became much broader in Fig. 14, ball-like diamonds were deposited as shown in Fig. 15(b). This structure is often called a cauliflower structure because it looks similar to the vegetable cauliflower.

To explain such a size effect of CNPs on the microstructure evolution, weakening of bond strength by charge should be considered. In a soft charging condition such as thermal and hot wire CVD, which is in contrast with the hard charging condition in plasma CVD, most nanoparticles are expected to be singly charged. In this case, the charge effect on weakening of the bond strength would be diminished as the size increase. In other words, the smaller CNPs would more liquid-like than the larger ones. Therefore, large CNPs generated under the high methane concentration in Fig. 14 would be less liquid-like so that CNPs frequently fail to undergo epitaxial recrystallization, producing ball-like or cauliflower diamond structures as shown in Fig. 15(b). On the other hand small CNPs generated under the low methane concentration in Fig. 14 would be more liquid-like so that CNPs mostly undergo epitaxial recrystallization, producing high-quality diamonds with well-defined facets as shown in Figure 15(a).

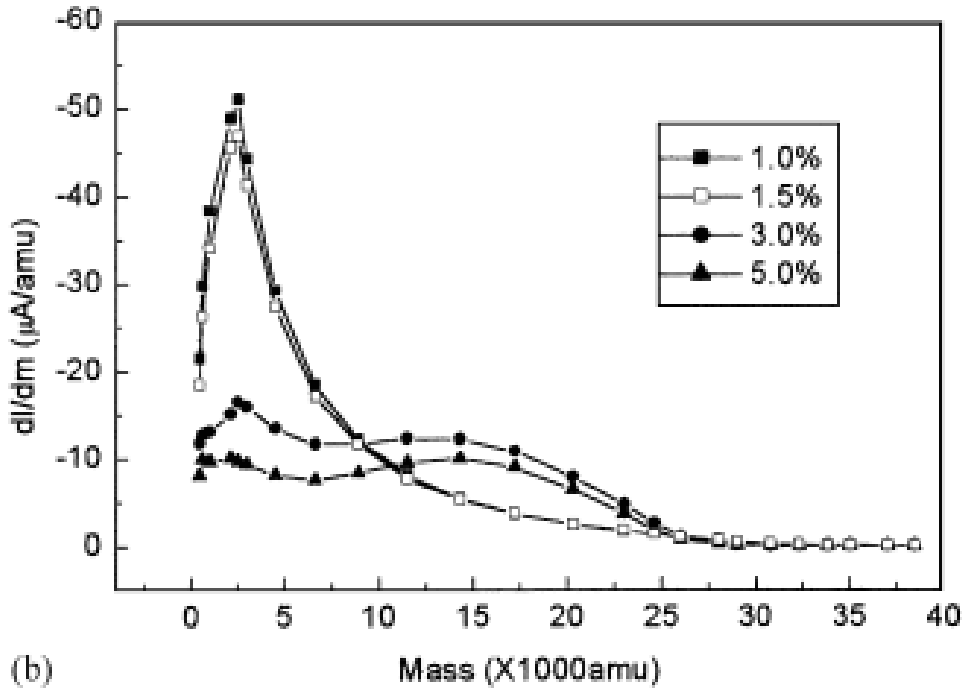

Fig. 14. Measured mass distributions of negatively charged carbon clusters extracted from the hot filament reactor using gas mixtures of 1%CH_4-99%H_2, 1.5%CH_4-98.5%H_2, 3%CH_4-97%H_2, and 5%CH_4-95%H_2 [7]

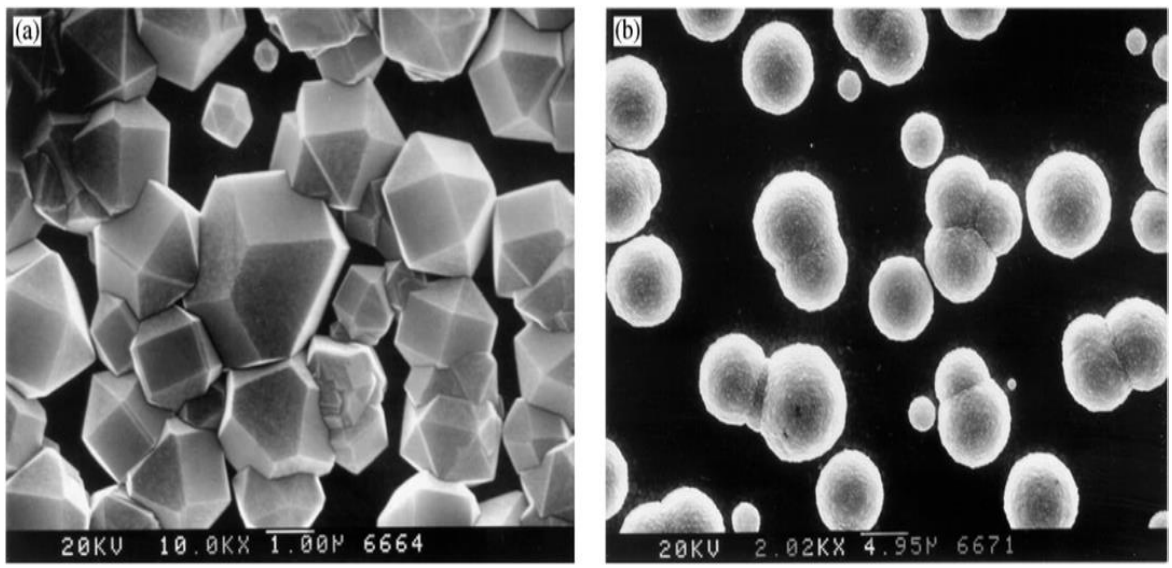

Fig.15. SEM images of diamond films deposited *in situ* during the measurement of the mass distribution of CNPs at 2100°C wire temperature and 800 Pa reactor pressure: (a) 1%CH_4–99%H_2, (b) 3%CH_4–97%H_2 [7]

To confirm the effect of nanoparticle size on the deposition behaviour, Yoshida and his colleagues [62-65] made extensive studies on the epitaxial growth of films with a building block of nanoparticles by the method called thermal plasma flash evaporation. They could deposit high-quality epitaxial $YBa_2Cu_3O_{7-x}$ films with a growth rate as high as 16 nm/s by this technique. They also could estimate the size of the nanoparticles to be about 0.3 – 10 nm by using a micro-trench fabricated on a Si wafer [66]. They observed that small 1–2 nm nanoparticles made epitaxial spiral growth, medium size 3 nm nanoparticles became epitaxial 2-dimensional particles, and large nanoparticles over 3 nm synthesised non-epitaxial island grains by scanning tunneling microscopy (STM) [62].

In general, deposited μc-Si:H films have inhomogeneous microstructure with vertical direction, even though high crystalline volume fraction of films could be obtained with high hydrogen dilution rate and substrate temperature. Amorphous incubation layer which has several tens to hundreds nanometers thick is inevitably deposited in the initial stage of the films. After then, microcrystalline phases are followed [67, 68]. Chung and Lee suggested that the one possibility for formation of such an inhomogeneous structure might be the flux change during deposition [69, 70]. Deposition flux in the initial stage might be factorable for the formation of the amorphous phase whereas that in the later stage might be favourable to microcrystalline phase. According to this possibility, it might be possible

to directly deposit μc-Si:H films after delaying deposition time artificially. From this idea, they shown that microcrystalline silicon was directly deposited on the glass substrate without amorphous incubation layer after appropriate delay time.

As mentioned earlier, that small CNPs are more liquid-like than large ones because the number of atoms per charge increases with increasing size of CNPs for the same amount of charge. Small CNPs favor the amorphous structure formation on glass and the epitaxial growth on a silicon wafer whereas large CNPs favor the microcrystalline structure formation on glass and the non-epitaxial growth on a silicon wafer. Therefore, the size of nanoparticles formed in the gas phase was crucial parameter of deposition.

2. Experimental concept of delay time

The concept of new possible processing parameter 'delay time' is originated from the puzzling microstructure of silicon films. Generally, cross sectional microstructure of the silicon film is vertically inhomogeneous. The AIL formed tens to hundreds nanometers in the initial stage and then, microcrystalline phases abruptly formed from the certain zone. This puzzling phenomenon means that the deposition flux could be charged during

deposition. In other words, size or phase of CNPs could be changed during deposition from the viewpoint of the TCN.

In this experiment, deposition delay time adopted to conform the deposition unit at the initial and later stage. Namely, size of nanoparticles could be confirmed by controlling the deposition delay time. HWCVD system with a shutter was used in this study. The shutter completely cover the substrate during reaction to delay the deposition. To control the delay time before deposition, a shutter, which covers a substrate and thereby isolates it from the reactor environment, was installed above the substrate as schematically shown in Fig. 16. The delay time means the amount of time duration that the shutter covered a substrate after the filaments were heated up in the HWCVD process.

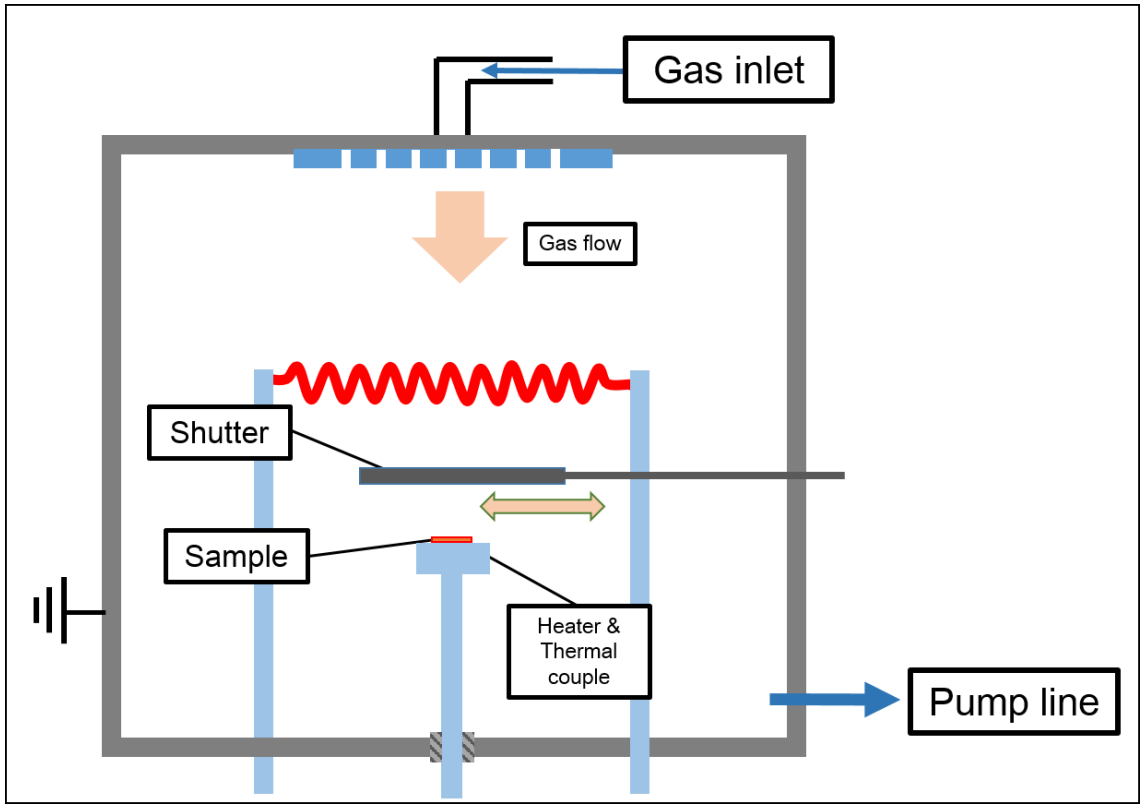

Fig.16. Schematic of experimental set-up of the HWCVD reactor.

Part 2. Experimental confirmation of behavior of charged nanoparticles during HW-CVD by capturing the particles.

1. Experimental details

Silicon thin films were deposited using an HWCVD reactor, where three linear tungsten filaments were aligned in parallel. The distance between the substrate and filament was 2 cm. The temperatures of the filament and substrate were measured respectively by an infrared optical pyrometer and the direct contact of a thermocouple with the substrate. The substrate temperature was controlled with a self-regulating heating system. The filament and substrate temperatures were respectively 1800℃ and 500 ℃. The reactor pressure was 13.3 Pa. The flow rate of each precursor and gas was controlled by a mass flow controller (MFC, Tylan). Hydrogen (H_2) diluted 30 vol% silane (SiH_4 99.9999%, Wonik materials), and 5 vol% phosphine (PH_3, 99.9999% Air liquid) gases were used as a precursor for n-type doping to measure the electrical property. The flow rates of H_2 diluted SiH_4, H_2 diluted PH_3 and H_2 were fixed at 5 sccm, 1.6 sccm and 12 sccm, respectively. To improve the crystallinity of films, 24 sccm of HCl (99.999% Tsurumi

Soda) was supplied [26-28].

To confirm how the size of nanoparticles formed in the gas phase varies with delay time, the nanoparticles were captured for 10 sec on a carbon membrane of the TEM Cu grid using a shutter after delay times of 0, 5 and 15 min and observed by TEM. To examine the effect of the size of nanoparticles on the deposition behavior, it is necessary to deposit the relatively uniform size of nanoparticles. However, the size of nanoparticles continues to increase with processing time until it reaches a steady state value after ~15 min in this process of HWCVD. For this reason, it is not possible to deposit films exclusively with small nanoparticles which are generated in the initial stage of deposition.

2. Result and discussion

Figs. 17(a)-(c) show the CNPs captured for 10 sec on a carbon membrane of the Cu TEM grid respectively after delay times of 0, 5 and 15 min. The size of the silicon CNPs increases with increasing delay time. The size tends to be saturated after a delay time of 15 min. This means that the CNPs continue to grow up to 15 min in the gas phase with the processing time of HWCVD and the steady state is reached at around 15 min. In other words, if the deposition is made as soon as the filament is heated up, which corresponds to the delay time of 0 min, the small CNPs, whose size is shown in Fig. 17(a), would land

initially on the substrate. As the deposition goes on, the CNPs would grow in the gas phase and the larger CNPs would land on the growing surface. This means that the size of CNPs to be deposited would continue to increase up to 15 min, where the steady state is reached.

If the deposition is made after the delay time of 5 min, the CNPs, whose size is shown in Fig. 17(b), would land on the substrate. Further, if the deposition is made after the delay time of 15 min, the CNPs, whose size is shown in Fig. 17(c), would land on the substrate. Therefore, the size of CNPs in their initial stage of deposition can be controlled by the delay time. In this sense, the delay time can be a new deposition parameter

According to Fig. 17, the size of CNPs increases with deposition time up to 15 min. Therefore, CNPs would have a minimum size in the initial stage of deposition and be liquid-like. After the initial stage of deposition, the size of CNPs is increasing with increase deposition time and CNPs are solid-like.

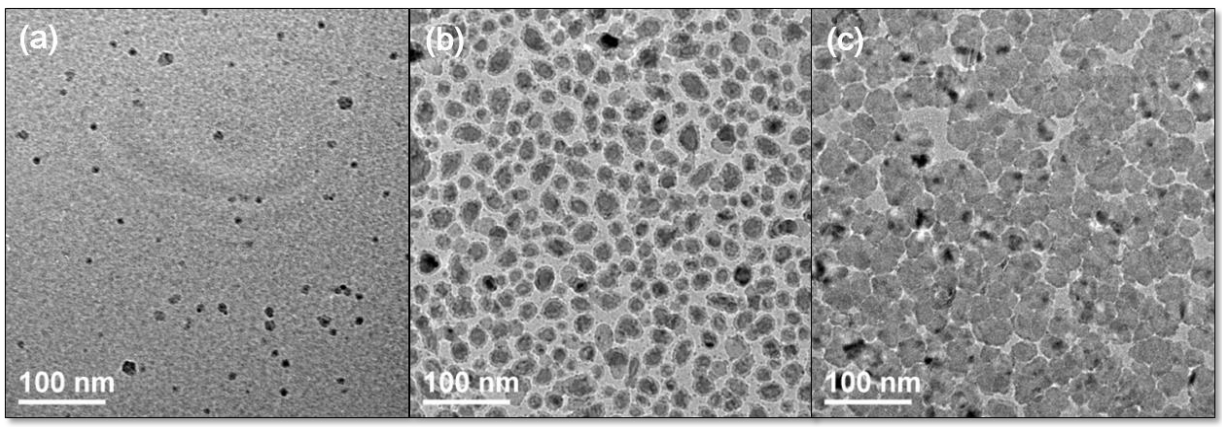

Fig. 17. TEM image of initial silicon charged nanoparticles deposited on the TEM grid membrane for 10 sec after delay times of (a) 0 min and (b) 5 min and (c) 15 min.

\

3. Conclusion

The size of nanoparticles formed in the gas phase was shown to increase with deposition time up to 15 min. This tendency is represented the delay time could be a new parameter of deposition during CVD reactor.

Part 3. Homo-epitaxial growth of silicon films during HWCVD

1. Experimental details

Silicon thin films were deposited using an HWCVD reactor, where three linear tungsten filaments were aligned in parallel. The distance between the substrate and filament was 2 cm. The temperatures of the filament and substrate were measured respectively by an infrared optical pyrometer and the direct contact of a thermocouple with the substrate. The substrate temperature was controlled with a self-regulating heating system. The filament and substrate temperatures were respectively 1800℃ and 600 ℃. The reactor pressure was 13.3 Pa. The flow rate of each precursor and gas was controlled by a mass flow controller (MFC, Tylan). Hydrogen (H_2) diluted 30 vol% silane (SiH_4 99.9999%, Wonik materials), were used as a precursor for n-type doping to measure the electrical property. . In order to examine the size effect of nanoparticles on the homo-epitaxial growth on p-type (100) silicon wafers during HWCVD, the cyclic process was used to deposit the film exclusively with the small nanoparticles generated for the first 30 sec. The deposition behavior was compared with that of the normal deposition process. For epitaxial growth, the silicon

wafers were pretreated by dipping in a 5 % HF solution in order to remove an organic residues and a native oxide. To decrease the size of nanoparticles further, the flow rates of hydrogendiluted 30 % SiH_4 and HCl were 2.5 sccm and 11 sccm, respectively. The distance between the substrate and filament was 3 cm. Also the filament and substrate temperatures were fixed respectively at 1800 ℃ and 600 ℃.

Since the size of CNPs tends to be minimum at the beginning of the process and continues to increase with processing time, the deposition with the minimum size of CNPs would be possible only at the beginning of the process. Therefore, in order to deposit films exclusively with the minimum size, a special method such as the cyclic process shown in Fig. 18(d) should be used.

Considering the liquid-like property of small CNPs, the deposition condition of Fig. 18(d), where only small CNPs are supplied, would be most favorable for epitaxial growth although it produced the lowest crystalline fraction on an amorphous glass substrate. In order to test this possibility, the deposition behavior on a single crystalline p-type (100) silicon wafer was compared between two deposition conditions. One is the normal deposition condition shown in Fig. 18(a).

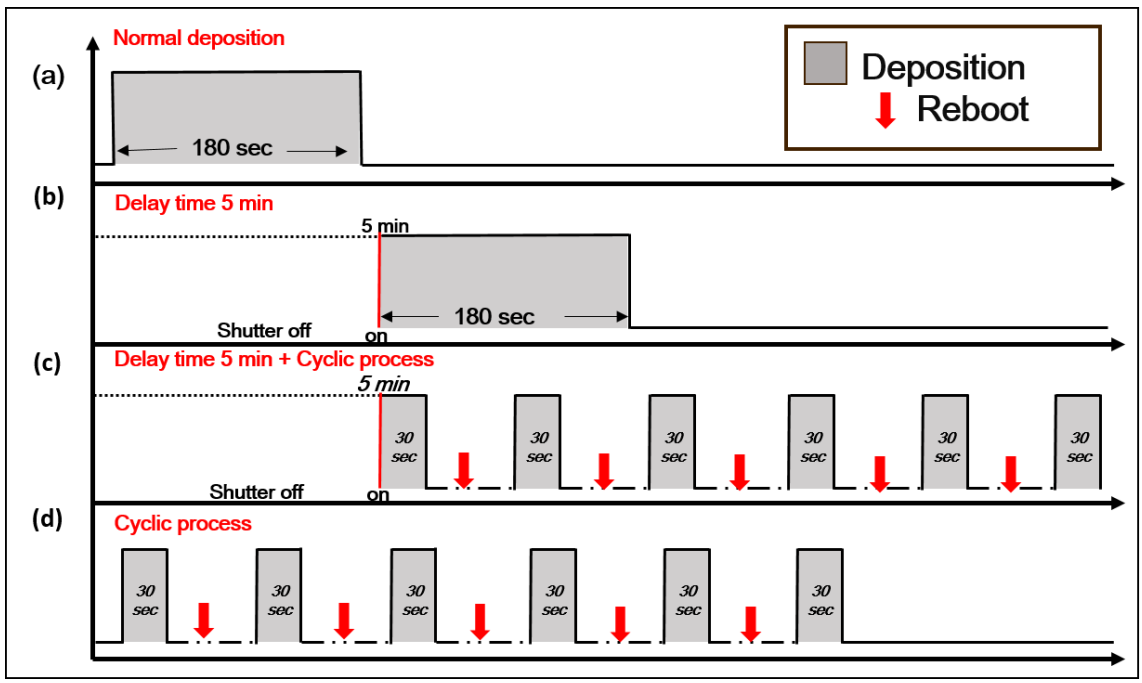

Fig. 18. Schematics of experimental deposition conditions of silicon films. (a) Normal deposition without delay time, (b) deposition with delay time, (c) after delay time for 5 min, 6 times of cyclic deposition process for 30 sec, and (d) 6 times of cyclic deposition process for 30 sec without delay time.

2. Result and discussion

Fig. 7 shows that TEM images of the silicon film deposited on a silicon wafer by the normal condition shown in Fig. 2(a), where the deposition was done for 180 sec without a delay time. Fig. 7(a) shows an overall cross section image of the film. The film thickness is ~ 150 nm. This image consists of three layers distinguished by the contrast. The lower dark layer is the silicon wafer with the middle black and the upper dark layers being the deposited silicon film. HRTEM images of the upper dark and the middle black layers, which are indicated by the square in Fig. 7(a), are shown respectively in Figs. 7(b) and 7(c). The HRTEM image of the upper dark layer shows typical microcrystalline silicon as revealed also by the diffraction pattern in the inset of Fig. 7(b). The HRTEM image of the middle black layer shows the epitaxial growth on the wafer. However, the epitaxial growth breaks down abruptly above the black layer and the microstructure changes to the upper dark layer of microcrystalline silicon. Fig. 8 shows TEM images of the silicon film deposited on a silicon wafer by the deposition condition shown in Fig. 2(d), where the film was prepared by the 6 times of cyclic deposition process for 30 sec with the total deposition time being 180 sec. Fig. 8(a) shows an overall cross section image of the film. The thickness of the film is ~ 150 nm. This image consists of two layers distinguished by the

contrast. The lower white layer is the silicon wafer with the upper gray layer being the deposited silicon film. HRTEM images of the upper and the interfacial layers, which are indicated by the square in Fig. 8(a), are shown respectively in Figs. 8(b) and 8(c). Figs. 8(b) and 8(c) show that a fully homo-epitaxial silicon film was grown on the silicon wafer substrate although there exist some stacking faults. To grow an epitaxial film, CNPs should be made as liquid-like as possible. To achieve this condition, the size of CNPs should be minimized and the substrate temperature should be increased. To decrease the size of CNPs, the cyclic deposition process shown in Fig. 2(d) can be used or the flow rate of the reactant gases can be decreased. For example, the deposition condition of Fig. 2(d) combined with the increased substrate temperature and the decreased flow rate of reactant gases resulted in successful epitaxial growth as shown in Fig. 8.

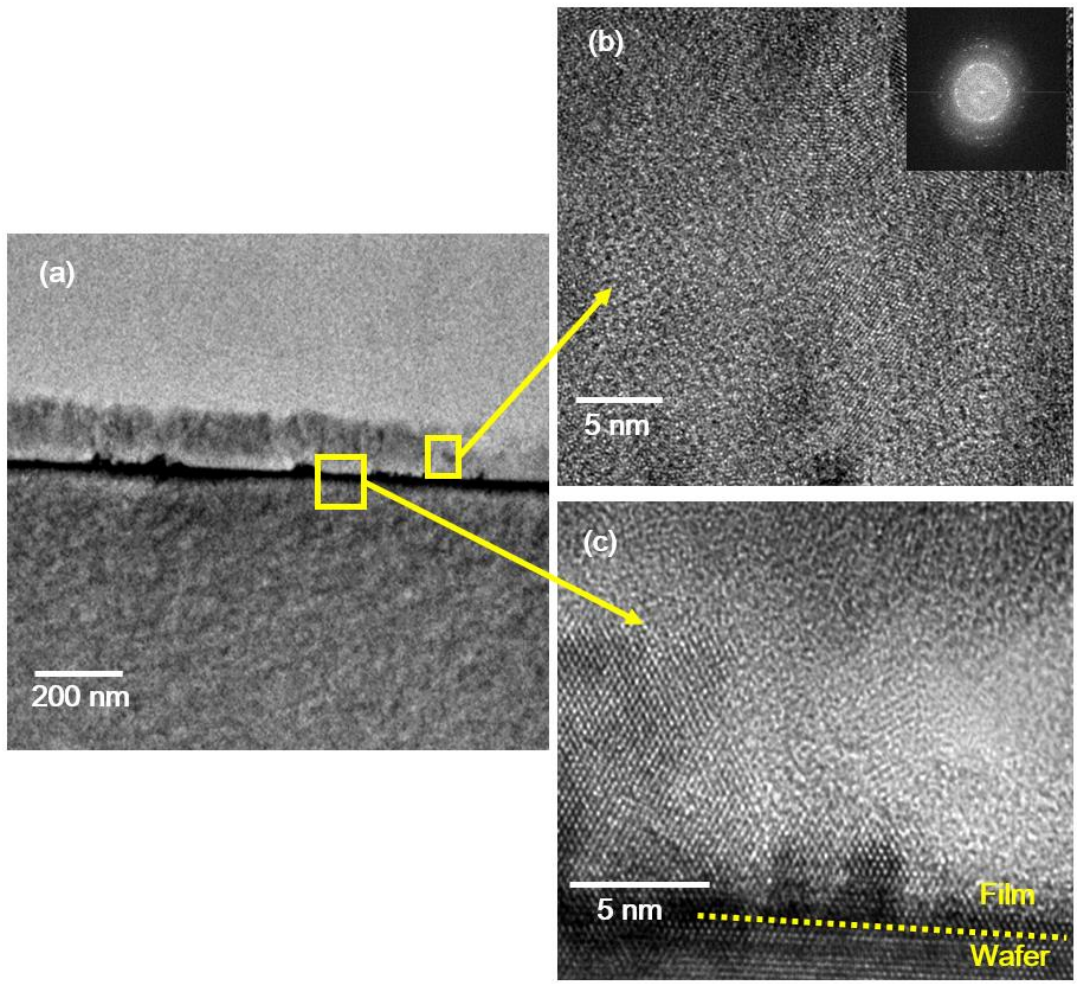

Fig. 19. TEM cross section images of the silicon film deposited on (100) silicon wafer under the normal condition without delay time. (a) Low magnification TEM image, (b) HRTEM image of the upper dark region, and (c) HRTEM image of the interfacial region between the silicon wafer and the lower dark region

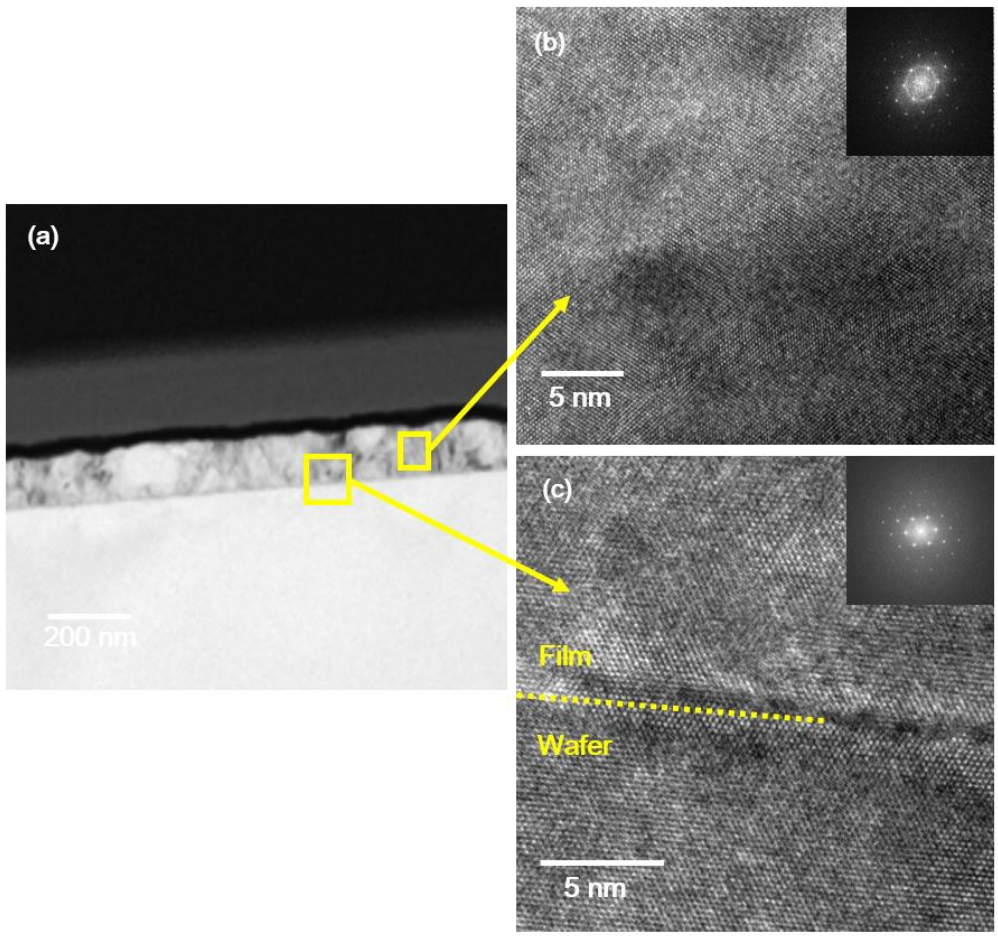

Fig. 20. TEM cross section images of the silicon film deposited on (100) silicon wafer under the condition of Figure 2(d) with 6 times of the cyclic deposition process for 30 sec. (a) Low magnification TEM image of films, (b) HRTEM image of the upper gray layer, and (c) HRTEM image of the interfacial region between the silicon wafer and the film.

3. Conclusion

Effect of size of CPNs on the homo-epitaxial growth of silicon film was studied based on the understanding of small size CNP's liquid like property in diffusion. To deposit the epitaxial silicon films, small size CNPs which formed in the initial growth stage continuously supplied. This result could be one of the critical experimental evidence for charge enhanced diffusion.

Chapter 4. Summary and conclusion

Silicon thin films have been extensively used in electrical devices for thin film transistor (TFTs) and silicon thin film based solar cells. But when it fabricated at low temperature, it is hard to obtain the high quality epitaxial silicon thin films. Because, diffusivity of silicon atom is very low at that temperature. By the reason, epitaxial silicon thin films are less applied in the industry than amorphous or microcrystalline silicon films.

Until now, deposition of nanostructure or films explained by classical crystallization based on atomic or molecules growth. However, there have been experimental results, which cannot be properly explained by this classical crystallization [8, 45]. Rather such experimental results imply that nanostructure or films should be grown by the growth unit of nanoparticles, whose way of crystal growth is called 'non-classical crystallization'

Based on the understanding of non-classical crystallization, epitaxial silicon films were deposited in the RF-PECVD and HWCVD systems. During RF-PECVD, homo and hetero epitaxial silicon films could be deposited at 550 ℃ by negative substrate bias. The deposition behavior and deposition rates depended on the substrate bias. Multiply CNPs, which were attracted by negative substrate bias, favor the silicon epitaxial films. This deposition behavior of films can be applied to the low temperature epitaxial film growth.

During HWCVD, based on the understanding of small size CNP's liquid like property, homo epitaxial silicon films were deposited and mechanism of deposition was studied.The development of thin technology should allow the deposition of high quality epitaxial film at low temperature.

These results indicate the growth unit of deposition in the RF-PECVD and HWCVD was CNPs and diffusivity of nanoparticles could be enhanced by charge. By the reason, substrate bias and size of CNPs can be a crucial deposition parameters in the various CVD processes.

Reference

[1] L. Boufendi, A. Plain, J.P. Blondeau, A. Bouchoule, C. Laure, M. Toogood, Measurements of particle size kinetics from nanometer to micrometer scale in a low-pressure argon-silane radio-frequency discharge, Applied Physics Letters, 60 (1992) 169.

[2] A.A. Howling, L. Sansonnens, J.L. Dorier, C. Hollenstein, Negative Hydrogenated Silicon Ion Clusters as Particle Precursors in Rf Silane Plasma Deposition Experiments, J Phys D Appl Phys, 26 (1993) 1003-1006.

[3] S. Veprek, O. Ambacher, W. Rieger, K. Schopper, M.G.J. Veprek-Heijman, Clusters in a silane glow discharge: Mechanism of their formation and how to avoid them, in: Materials Research Society Symposium Proceedings, 1993, pp. 13-18.

[4] A. Garscadden, B.N. Ganguly, P.D. Haaland, J. Williams, Overview of growth and behaviour of clusters and particles in plasmas, Plasma Sources Sci T, 3 (1994) 239-245.

[5] E. Stoffels, W.W. Stoffels, G.M.W. Kroesen, F.J. deHoog, Dust formation and charging in an Ar/SiH4 radio-frequency discharge, Journal of Vacuum Science & Technology a-Vacuum Surfaces and Films, 14 (1996) 556-561.

[6] N.M. Hwang, D.K. Lee, Charged nanoparticles in thin film and nanostructure growth by chemical vapour deposition, Journal of Physics D: Applied Physics, 43 (2010).

[7] J.S. Jung, N.M. Hwang, Non-classical crystallization of thin films and nanostructures in CVD process, in: S. Neralla (Ed.) Chemical vapor deposition, Intech, USA, 2016.

[8] N.M. Hwang, D.Y. Yoon, Thermodynamic approach to the paradox of diamond formation with simultaneous graphite etching in the low pressure synthesis of diamond, Journal of Crystal Growth, 160 (1996) 98-103.

[9] N.M. Hwang, J.H. Hahn, D.Y. Yoon, Charged cluster model in the low pressure synthesis of diamond, Journal of Crystal Growth, 162 (1996) 55-68.

[10] N.M. Hwang, J.H. Hahn, D.Y. Yoon, Chemical potential of carbon in the low pressure synthesis of diamond, Journal of Crystal Growth, 160 (1996) 87-97.

[11] N.M. Hwang, D.Y. Kim, Charged clusters in thin film growth, International Materials Reviews, 49 (2004) 171-190.

[12] J.D. Jeon, C.J. Park, D.Y. Kim, N.M. Hwang, Experimental confirmation of charged carbon clusters in the hot filament diamond reactor, Journal of Crystal Growth, 213 (2000) 79-82.

[13] H.S. Ahn, H.M. Park, D.Y. Kim, N.M. Hwang, Observation of carbon clusters of a few nanometers in the oxyacetylene diamond CVD process, Journal of Crystal Growth, 234 (2002) 399-403.

[14] I.D. Jeon, L. Gueroudji, D.Y. Kim, N.M. Hwang, Temperature Dependence of the Deposition Behavior of Yttria-stabilized Zirconia CVD Films: Approach by Charged Cluster Model, Journal of the Korean Ceramic Society, 38 (2001) 218-224.

[15] J.Y. Kim, D.Y. Kim, N.M. Hwang, Spontaneous generation of negatively charged clusters and their deposition as crystalline films during hot-wire silicon chemical vapor deposition, Pure and Applied Chemistry, 78 (2006) 1715-1722.

[16] J.I. Lee, N.M. Hwang, Generation of negative-charge carriers in the gas phase and their contribution to the growth of carbon nanotubes during hot-filament chemical vapor deposition, Carbon, 46 (2008) 1588-1592.

[17] C.S. Kim, Y.B. Chung, W.K. Youn, N.M. Hwang, Generation of charged nanoparticles during the synthesis of carbon nanotubes by chemical vapor deposition, Carbon, 47 (2009) 2511-2518.

[18] C.S. Kim, Y.B. Chung, W.K. Youn, N.M. Hwang, Generation of charged nanoparticles during synthesis of ZnO nanowires by carbothermal reduction, Aerosol Science and Technology, 43 (2009) 120-125.

[19] C.S. Kim, I.J. Kwak, K.J. Choi, J.G. Park, N.M. Hwang, Generation of charged nanoparticles during the synthesis of silicon nanowires by chemical vapor deposition, Journal of Physical Chemistry C, 114 (2010) 3390-3395.

[20] P. Hartman, Crystal Growth: An Introduction, North Holland, Amsterdam, 1973.

[21] J.P. Van Der Eerden, Handbook of Crystal Growth Vol. 1a: Bulk Fundamentals, Growth Thermodynamics and Kinetics, North-Holland, Amsterdam, 1994.

[22] P.H. McMurry, D.J. Rader, Aerosol wall losses in electrically charged chambers, Aerosol Science and Technology, 4 (1985) 249-268.

[23] P. Roca i Cabarrocas, Plasma enhanced chemical vapor deposition of amorphous, polymorphous and microcrystalline silicon films, Journal of Non-Crystalline Solids, 266–269, Part 1 (2000) 31-37.

[24] P. Roca i Cabarrocas, Plasma enhanced chemical vapor deposition of silicon thin films for large

area electronics, Current Opinion in Solid State and Materials Science, 6 (2002) 439-444.

[25] S.V. Vladimirov, K. Ostrikov, Dynamic self-organization phenomena in complex ionized gas systems: New paradigms and technological aspects, Physics Reports, 393 (2004) 175-380.

[26] S. Nunomura, K. Koga, M. Shiratani, Y. Watanabe, Y. Morisada, N. Matsuki, S. Ikeda, Fabrication of nanoparticle composite porous films having ultralow dielectric constant, Japanese Journal of Applied Physics, Part 2: Letters, 44 (2005) L1509-L1511.

[27] A. Glasner, J. Kenat, The crystallization of KCl from aqueous solutions in the presence of lead ions. I. A calorimetric study, Journal of Crystal Growth, 2 (1968) 119-127.

[28] A. Glasner, S. Skurnik, A New Mechanism for the Crystallization and Growth of Ionic Crystals, with Special Reference to KCl in the Presence of Pb2+Ions, Israel J. Chem., 6 (1968).

[29] A. Glasner, M. Tassa, The Thermal Effects of Nucleation and Crystallization of KBr and KCl Solutions. II. The Heat Of Nucleation and the Supersaturated Solution, Israel Journal of Chemistry, 12 (1974) 799-816.

[30] A. Glasner, M. Tassa, The Thermal Effects of Nucleation and Crystallization of KBr and KCl Solutions. II. The Heat Of Nucleation and the Supersaturated Solution, Israel J. Chem., 12 (1974) 799-816.

[31] G.D. Botsaris, R.C. Reid, Comments on the Letter by Glasner and Skurnik Entitled ``Growth of Potassium Chloride Crystals from Aqueous Solutions. I. The Effect of Lead Chloride", J. Chem. Phys., 47 (1967) 3689-3690.

[32] R.E.I. Schropp, Status of Cat-CVD (Hot-Wire CVD) research in Europe, Thin Solid Films, 395

(2001) 17-24.

[33] A. Shah, Thin-film silicon solar cells, Thin-Film Silicon Solar Cells, (2010).

[34] R. Prasad, S.R. Shenoy, Staebler-Wronski effect in hydrogenated amorphous silicon, Physics Letters A, 218 (1996) 85-90.

[35] H. Wiesmann, A.K. Ghosh, T. McMahon, M. Strongin, A-Si : H produced by high-temperature thermal decomposition of silane, Journal of Applied Physics, 50 (1979) 3752-3754.

[36] D. J., Production of high-quality amorphous silicon films by evaporative silane surface decomposition method using intermediate species SiF2, Journal of Applied Physics, 64 (1988) 3215.

[37] H. Matsumura, Formation of silicon-based thin films prepared by Catalytic Chemical Vapor Deposition (Cat-CVD) method, Japanese Journal of Applied Physics, Part 1: Regular Papers and Short Notes and Review Papers, 37 (1998) 3175-3187.

[38] A.H. Mahan, J. Carapella, B.P. Nelson, R.S. Crandall, I. Balberg, Deposition of device quality, low H content amorphous silicon, Journal of Applied Physics, 69 (1991) 6728-6730.

[39] H. Matsumura, Formation of polysilicon films by catalytic chemical vapor deposition (cat-CVD) method, Japanese Journal of Applied Physics, Part 2: Letters, 30 (1991) L1522-L1524.

[40] E. Persidis, H. Baur, F. Pieralisi, P. Schalberger, N. Fruehauf, Area laser crystallized LTPS TFTs with implanted contacts for active matrix OLED displays, Solid-State Electronics, 52 (2008) 455-461.

[41] S. Uchikoga, N. Ibaraki, Low temperature poly-Si TFT-LCD by excimer laser anneal, Thin Solid Films, 383 (2001) 19-24.

[42] A. Shah, P. Torres, R. Tscharner, N. Wyrsch, H. Keppner, Photovoltaic technology: The case for thin-film solar cells, Science, 285 (1999) 692-698.

[43] H. Kahn, N. Tayebi, R. Ballarini, R.L. Mullen, A.H. Heuer, Fracture toughness of polysilicon MEMS devices, Sensors and Actuators, A: Physical, 82 (2000) 274-280.

[44] J.P. Van Der Eerden, Crystal growth mechanisms, Handbook of Crystal Growth, 1 (1993).

[45] J.H. Hahn, N.M. Hwang, D.Y. Yoon, Formation of soot or diamond on the iron substrate in the chemical vapour deposition process of diamond, Journal of Materials Science Letters, 15 (1996) 1240-1242.

[46] C.S. Kim, W.K. Youn, N.M. Hwang, Generation of charged nanoparticles and their deposition during the synthesis of silicon thin films by chemical vapor deposition, Journal of Applied Physics, 108 (2010).

[47] W.K. Youn, C.S. Kim, J.Y. Lee, S.S. Lee, N.M. Hwang, Generation of charged nanoparticles and their deposition behavior under alternating electric bias during chemical vapor deposition of silicon, Journal of Physical Chemistry C, 116 (2012) 25157-25163.

[48] S.S. Lee, M.S. Ko, C.S. Kim, N.M. Hwang, Gas phase nucleation of crystalline silicon and their role in low-temperature deposition of microcrystalline films during hot-wire chemical vapor deposition, Journal of Crystal Growth, 310 (2008) 3659-3662.

[49] J.S. Hong, C.S. Kim, S.W. Yoo, S.H. Park, N.M. Hwang, H.M. Choi, D.B. Kim, T.S. Kim, In-Situ measurements of charged nanoparticles generated during hot wire chemical vapor deposition of silicon using particle beam mass spectrometer, Aerosol Science and Technology, 47 (2013) 46-

51.

[50] S.S. Lee, C.S. Kim, N.M. Hwang, Generation of charged nanoparticles during the synthesis of GaN nanostructures by atmospheric-pressure chemical vapor deposition, Aerosol Science and Technology, 46 (2012) 1100-1108.

[51] P. Roca I Cabarrocas, Plasma enhanced chemical vapor deposition of amorphous, polymorphous and microcrystalline silicon films, Journal of Non-Crystalline Solids, 266-269 A (2000) 31-37.

[52] A. Fontcuberta i Morral, P. Roca i Cabarrocas, Etching and hydrogen diffusion mechanisms during a hydrogen plasma treatment of silicon thin films, Journal of Non-Crystalline Solids, 299-302 (2002) 196-200.

[53] P.R.I. Cabarrocas, N. Chaâbane, A.V. Kharchenko, S. Tchakarov, Polymorphous silicon thin films produced in dusty plasmas: Application to solar cells, Plasma Physics and Controlled Fusion, 46 (2004) B235-B243.

[54] T.G. Clare B W, Jennings P J, Cornish J C L, Hefter G T. , Effect of charge on bond strength in hydrogenated amorphous silicon, J. Comp. Chem. , 15 (1994) 644.

[55] B. Zheng, Y.Y. Wu, P.D. Yang, J. Liu, Synthesis of ultra-long and highly oriented silicon oxide nanowires from liquid alloys, Advanced Materials, 14 (2002) 122-+.

[56] H.Y. Zhao, Q.L. Fan, L.X. Song, T. Zhang, E.W. Shi, X.F. Hu, Synthesis and characterization of superhard Ti-Si-N films obtained in an inductively coupled plasma enhanced chemical vapor deposition (ICP-CVD) with magnetic confinement, Applied Surface Science, 252 (2006) 3065-

3072.

[57] L.W. Yin, M.S. Li, D.S. Sun, F.Z. Li, Z.Y. Hao, Some aspects of diamond crystal growth at high temperature and high pressure by TEM and SEM, Materials Letters, 55 (2002) 397-402.

[58] N.M. Hwang, W.S. Cheong, D.Y. Yoon, Deposition Behaviors of Si on Insulating and Conducting Substrates in the CVD Process: Approach by Charged Cluster Model, J. Cryst. Growth, 206 (1999) 177-186.

[59] J.K. Rath, B. Stannowski, P.A.T.T. Van Veenendaal, M.K. Van Veen, R.E.I. Schropp, Application of hot-wire chemical vapor-deposited Si:H films in thin film transistors and solar cells, Thin Solid Films, 395 (2001) 320-329.

[60] A.V. Shah, J. Meier, E. Vallat-Sauvain, N. Wyrsch, U. Kroll, C. Droz, U. Graf, Material and solar cell research in microcrystalline silicon, Solar Energy Materials and Solar Cells, 78 (2003) 469-491.

[61] J.M. Huh, D.Y. Yoon, D.Y. Kim, N.M. Hwang, Effect of substrate materials in the low-pressure synthesis of diamond: Approach by theory of charged clusters, Zeitschrift fuer Metallkunde/Materials Research and Advanced Techniques, 96 (2005) 225-232.

[62] K. Hayasaki, Y. Takamura, N. Yamaguchi, K. Terashima, T. Yoshida, Scanning tunneling microscopy of epitaxial YBa2Cu3O7-x films prepared by thermal plasma flash evaporation method, Journal of Applied Physics, 81 (1997) 1222-1226.

[63] Y. Takamura, K. Hayasaki, K. Terashima, T. Yoshida, Cluster size measurement using microtrench in a thermal plasma flash evaporation process, Journal of Vacuum Science and

Technology B: Microelectronics and Nanometer Structures, 15 (1997) 558-565.

[64] Y. Takamura, N. Yamaguchi, K. Terashima, T. Yoshida, High-rate deposition of YBa2Cu3O7-x films by hot cluster epitaxy, Journal of Applied Physics, 84 (1998) 5084-5088.

[65] N. Yamaguchi, Y. Sasajima, K. Terashima, T. Yoshida, Molecular dynamics study of cluster deposition in thermal plasma flash evaporation, Thin Solid Films, 345 (1999) 34-37.

[66] Y. Takamura, K. Hayasaki, K. Terashima, T. Yoshida, Cluster size measurement using microtrench in a thermal plasma flash evaporation process, J Vac Sci Technol B, 15 (1997) 558-565.

[67] J.K. Rath, Low temperature polycrystalline silicon: A review on deposition, physical properties and solar cell applications, Solar Energy Materials and Solar Cells, 76 (2003) 431-487.

[68] S.W. Choi, K.J. Bachmann, G. Lucovsky, Growth-Kinetics and Characterizations of Gallium Nitride Thin-Films by Remote Pecvd, Journal of Materials Research, 8 (1993) 847-854.

[69] Y.B. Chung, D.K. Lee, C.S. Kim, N.M. Hwang, Effect of HCl addition on the crystalline fraction in silicon thin films prepared by hot-wire chemical vapor deposition, Vacuum, 83 (2009) 1431-1434.

[70] Y.B. Chung, H.K. Park, D.K. Lee, W. Jo, J.H. Song, S.H. Lee, N.M. Hwang, Low temperature deposition of crystalline silicon on glass by hot wire chemical vapor deposition, Journal of Crystal Growth, 327 (2011) 57-62.

국문 초록

실리콘박막은 현재 박막 트랜지스터나 실리콘 박막 태양전지 등 다양한 전자 제품에 널리 사용되고 있다. 그러나 이러한 실리콘 박막의 사용은 비정질이나 결정질 실리콘 박막에만 국한되며 가장 물성이 좋은 단결정 실리콘 박막은 현재 산업적으로 거의 사용되지 않고 있다. 이는 단결정 실리콘 박막의 증착의 어려움 때문이다. 따라서 본 연구에서는 이러한 단결정 실리콘 박막을 새로운 박막 증착에 관한 이해인 비고전적 박막 증착에 기반하여 보다 간단하고 낮은 공정비용으로 증착 가능한 공정을 개발하는 것을 목표로 한다. 기존의 박막 및 나노구조체에 관련된 연구는 원자가 분자가 그 증착 단위가 된다는 고전적 박막성장 이론을 주로 믿어왔다. 그러나 이러한 고전적 박막 증착으로는 설명되지 않는 다양한 연구결과가 나타남에 따라 원자가 분자가 아닌 기상에서 생성된 하전을 띈 나노입자가 박막 및 나노 구조체의 증착 단위가 된다는 비고전적 박막 성장에 관한 연구가 점차 늘어났고 이를 통해 기존에 설명이 불가능했던 현상들을 설명하는 것이 가능해졌다. 이러한 비고전적 박막 성장에 따르면 기상의 존재하는 입자는 그 크기가 작을수록, 하전을 많

이 가질수록 입자의 확산이 활성화되며 즉, 이러한 입자는 단결정 성장에 유리하게 된다.

본 연구에서는 이러한 비고전적 박막 성장 이론에 기반하여 라디오 주파수 영역 플라즈마 화학 기상 증착공정(RF-PECVD)과 열선 필라멘트 화학 기상 증착 공정(HWCVD)에서의 하전을 띈 나노입자의 공정 조건에 따른 거동을 분석한 후 이러한 거동을 이용하여 상대적으로 저온에서 간단한 공정을 통한 단결정 실리콘 박막을 증착하는 것을 목표로 한다.

RF-PECVD에서는 하전을 띈 나노입자를 기상에서 투과전자현미경용 그리드에 포집하여 기판 전압 및 그리드의 전도성에 따른 거동을 관찰하였고 그를 통해 음의 기판 전위 시 단결정 성장에 유리한 하전된 나노입자를 우선적으로 증착 시킬 수 있다는 것을 확인하였다. 또한 박막의 증착 속도 분석을 통해 이러한 기판 전압 효과가 증착 시간이 지날수록 전하 축적 현상에 의해 약화된다는 것을 관찰하였다. 이러한 성질을 이용하여 실리콘 웨이퍼 위에 상대적으로 저온인 기판온도 550도에서 단결정 실리콘 박막을 증착하는데 성공하였다.

HWCVD에서는 각 조건에 따른 입자 포집을 통해 기상에 존재하는 입자의 크기가 시간이 지날수록 증가한다는 것을 확인하였고 단결정 성장에 유리한 크기가 작은 입자만을 우선적으로 포집하는 조건을 수립하여 기판 온도 600 도에서 실리콘 웨이퍼 위에 단결정 실리콘 박막을 증착하는데 성공하였다.

본 연구를 통해 기존에 증착이 힘들었던 저온에서의 단결정 실리콘 박막 증착을 기판 전위와 입자 크기 조절을 통해 이룰 수 있었고 이러한 공정 변수들은 앞으로 단결정 성장뿐만이 아니라 박막 성장 전반에 있어서 고려해야 할 중요한 변수가 될 것이라 기대된다.

주요어 : 실리콘 박막; 라디오 주파수 영역 플라즈마 화학 기상 증착 공정; 열선 필라멘트 화학 기상 증착 공정; 단결정 박막; 비고전적 박막 성장

학번 : 2011-20668